On Particle-Based Modeling of Immersion Freezing

S. Arabas[1,2], J.H. Curtis[1], I. Silber[3], A. Fridlind[4], D.A Knopf[5] & N. Riemer[1]

1: atmos.illinois.edu
2: uj.edu.pl
3: met.psu.edu
4: giss.nasa.gov
5: stonybrook.edu

funding:
ASR Atmospheric System Research

14th Symposium on Aerosol-Cloud-Climate Interactions / 102nd AMS Annual Meeting

virtual, Jan 27 2022

super-particles as a probabilistic alternative to bulk or bin μ-physics

JAMES | Journal of Advances in Modeling Earth Systems

COMMISSIONED MANUSCRIPT

10.1029/2019MS001689

Confronting the Challenge of Modeling Cloud and Precipitation Microphysics

Hugh Morrison[1], Marcus van Lier-Walqui[2], Ann M. Fridlind[3], Wojciech W. Grabowski[1], Jerry Y. Harrington[4], Corinna Hoose[5], Alexei Korolev[6], Matthew R. Kumjian[4], Jason A. Milbrandt[7], Hanna Pawlowska[8], Derek J. Posselt[9], Olivier P. Prat[10], Karly J. Reimel[4], Shin-Ichiro Shima[11], Bastiaan van Diedenhoven[2], and Lulin Xue[1]

Key Points:

- Microphysics is an important component of weather and climate models, but its representation in current models is highly uncertain

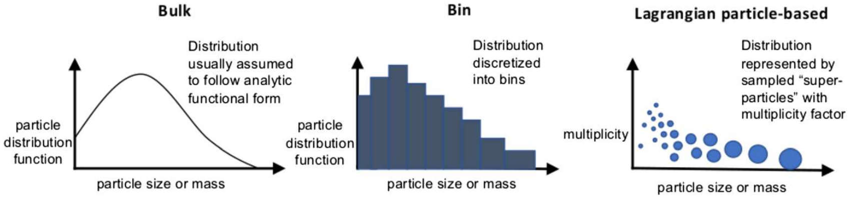

Figure 3. Representation of cloud and precipitation particle distributions in the three main types of microphysics

super-particles as a probabilistic alternative to bulk or bin μ-physics

JAMES Journal of Advances in Modeling Earth Systems

COMMISSIONED MANUSCRIPT
10.1029/2019MS001689

Key Points:
- Microphysics is an important component of weather and climate models, but its representation in current models is highly uncertain

Confronting the Challenge of Modeling Cloud and Precipitation Microphysics

Hugh Morrison[1], Marcus van Lier-Walqui[2], Ann M. Fridlind[3], Wojciech W. Grabowski[1], Jerry Y. Harrington[4], Corinna Hoose[5], Alexei Korolev[6], Matthew R. Kumjian[4], Jason A. Milbrandt[7], Hanna Pawlowska[8], Derek J. Posselt[9], Olivier P. Prat[10], Karly J. Reimel[4], Shin-Ichiro Shima[11], Bastiaan van Diedenhoven[2], and Lulin Xue[1]

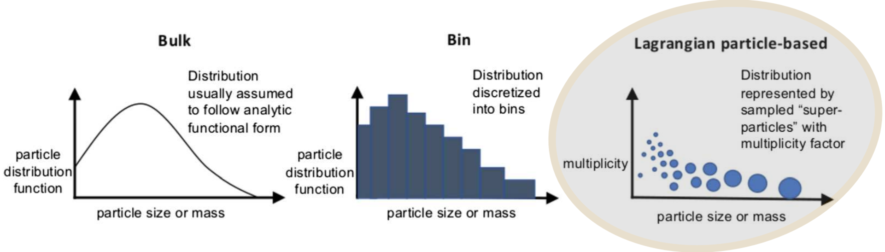

Figure 3. Representation of cloud and precipitation particle distributions in the three main types of microphysics

Shima, Sato, Hashimoto & Misumi 2020 (GMD):

Predicting the morphology of ice particles in deep convection using the super-droplet method

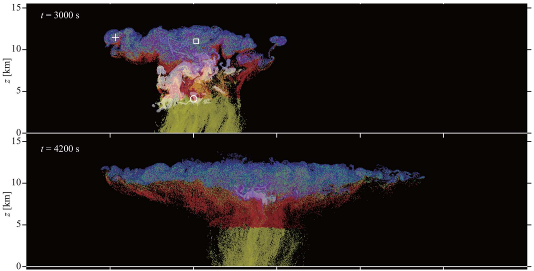

Figure 1. Typical realization of CTRL cloud spatial structures at $t = 2040$, 2460, 3000, 4200, and 5400 s. The mixing ratio of cloud water, rainwater, cloud ice, graupel, and snow aggregates are plotted in fading white, yellow, blue, red, and green, respectively. The symbols indicate examples of unrealistic predicted ice particles (Sects. 7.3 and 9.1). See also Movie 1 in the video supplement.

Shima et al. '20 particle-based mixed-phase μ-physics

Shima, Sato, Hashimoto & Misumi 2020 (GMD):
Predicting the morphology of ice particles in deep convection using the super-droplet method

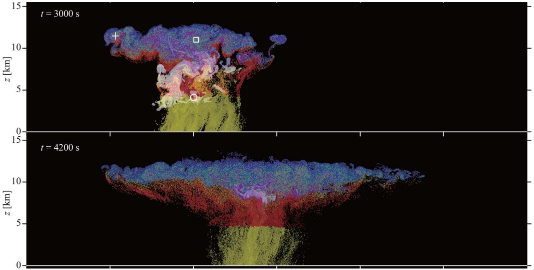

Figure 1. Typical realization of CTRL cloud spatial structures at $t = 2040$, 2460, 3000, 4200, and 5400 s. The mixing ratio of cloud water, rainwater, cloud ice, graupel, and snow aggregates are plotted in fading white, yellow, blue, red, and green, respectively. The symbols indicate examples of unrealistic predicted ice particles (Sects. 7.3 and 9.1). See also Movie 1 in the video supplement.

- Eulerian component: momentum, heat, moisture budget

Shima, Sato, Hashimoto & Misumi 2020 (GMD):

Predicting the morphology of ice particles in deep convection using the super-droplet method

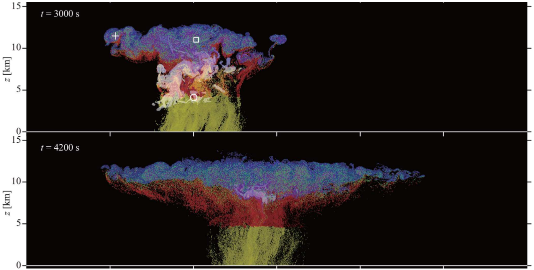

Figure 1. Typical realization of CTRL cloud spatial structures at $t = 2040$, 2460, 3000, 4200, and 5400 s. The mixing ratio of cloud water, rainwater, cloud ice, graupel, and snow aggregates are plotted in fading white, yellow, blue, red, and green, respectively. The symbols indicate examples of unrealistic predicted ice particles (Sects. 7.3 and 9.1). See also Movie 1 in the video supplement.

- Eulerian component: momentum, heat, moisture budget
- Lagrangian component: super particles representing aerosol, water droplets, ice particles (porous spheroids)

Shima et al. ’20 particle-based mixed-phase μ-physics

Shima, Sato, Hashimoto & Misumi 2020 (GMD):

Predicting the morphology of ice particles in deep convection using the super-droplet method

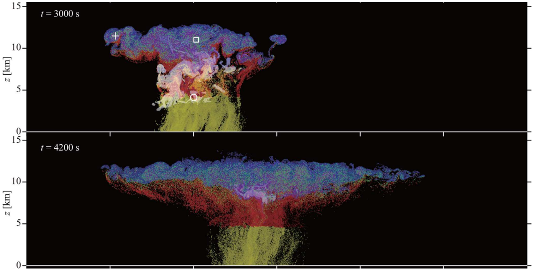

Figure 1. Typical realization of CTRL cloud spatial structures at $t = 2040$, 2460, 3000, 4200, and 5400 s. The mixing ratio of cloud water, rainwater, cloud ice, graupel, and snow aggregates are plotted in fading white, yellow, blue, red, and green, respectively. The symbols indicate examples of unrealistic predicted ice particles (Sects. 7.3 and 9.1). See also Movie 1 in the video supplement.

- Eulerian component: momentum, heat, moisture budget
- Lagrangian component: super particles representing aerosol, water droplets, ice particles (porous spheroids)

- particle-resolved processes:
  — advection and sedimentation
  — homogeneous and immersion freezing (singular)
  — melting
  — condensation and evaporation (incl. CCN [de]activation)
  — deposition and sublimation
  — collisions (coalescence, riming, aggregation, washout)

Shima, Sato, Hashimoto & Misumi 2020 (GMD):

Predicting the morphology of ice particles in deep convection using the super-droplet method

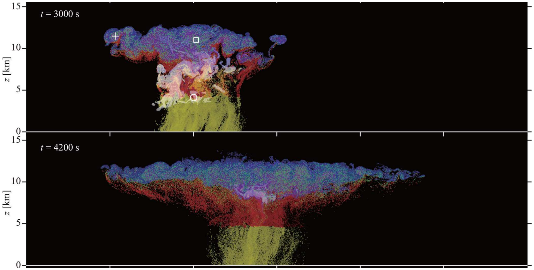

Figure 1. Typical realization of CTRL cloud spatial structures at $t = 2040$, 2460, 3000, 4200, and 5400 s. The mixing ratio of cloud water, rainwater, cloud ice, graupel, and snow aggregates are plotted in fading white, yellow, blue, red, and green, respectively. The symbols indicate examples of unrealistic predicted ice particles (Sects. 7.3 and 9.1). See also Movie 1 in the video supplement.

- Eulerian component: momentum, heat, moisture budget
- Lagrangian component: super particles representing aerosol, water droplets, ice particles (porous spheroids)
- particle-resolved processes:
  — advection and sedimentation
  — homogeneous and immersion freezing (singular)
  — melting
  — condensation and evaporation (incl. CCN [de]activation)
  — deposition and sublimation
  — collisions (coalescence, riming, aggregation, washout)
- 2D Cb test case with monodisperse INP

Shima et al. '20 particle-based mixed-phase μ-physics

Shima, Sato, Hashimoto & Misumi 2020 (GMD):

Predicting the morphology of ice particles in deep convection using the super-droplet method

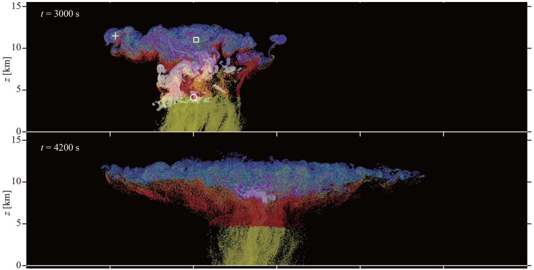

Figure 1. Typical realization of CTRL cloud spatial structures at $t = 2040$, 2460, 3000, 4200, and 5400 s. The mixing ratio of cloud water, rainwater, cloud ice, graupel, and snow aggregates are plotted in fading white, yellow, blue, red, and green, respectively. The symbols indicate examples of unrealistic predicted ice particles (Sects. 7.3 and 9.1). See also Movie 1 in the video supplement.

- Eulerian component: momentum, heat, moisture budget
- Lagrangian component: super particles representing aerosol, water droplets, ice particles (porous spheroids)
- particle-resolved processes:
  — advection and sedimentation
  — homogeneous and immersion freezing (singular)
  — melting
  — condensation and evaporation (incl. CCN [de]activation)
  — deposition and sublimation
  — collisions (coalescence, riming, aggregation, washout)
- 2D Cb test case with monodisperse INP

Poissonian model of freezing & Ice Nucleation Active Sites (INAS)

theory (in modern notation)
(Bigg '53, Langham & Mason '58, Carte '59, Marshall '61)

Poissonian model of freezing & Ice Nucleation Active Sites (INAS)

theory (in modern notation)
(Bigg '53, Langham & Mason '58, Carte '59, Marshall '61)

Poisson counting process with rate r:

$$P^*(\text{k events in time t}) = \frac{(rt)^k \exp(-rt)}{k!}$$

$$P(\text{one or more events in time t}) = 1 - P^*(k=0, t)$$

$$\ln(1-P) = -rt$$

Poissonian model of freezing & Ice Nucleation Active Sites (INAS)

theory (in modern notation)
(Bigg '53, Langham & Mason '58, Carte '59, Marshall '61)

Poisson counting process with rate r:

$$P^*(\text{k events in time t}) = \frac{(rt)^k \exp(-rt)}{k!}$$

$$P(\text{one or more events in time t}) = 1 - P^*(k=0, t)$$

$$\ln(1-P) = -rt$$

introducing $J_{\text{het}}(T)$, $T(t)$ and INP surface A:

$$\ln\left(1 - P(A,t)\right) = -A \underbrace{\int_0^t J_{\text{het}}(T(t'))\, dt'}_{I(T)}$$

Poissonian model of freezing & Ice Nucleation Active Sites (INAS)

theory (in modern notation)
(Bigg '53, Langham & Mason '58, Carte '59, Marshall '61)

Poisson counting process with rate r:

$$P^*(\text{k events in time t}) = \frac{(rt)^k \exp(-rt)}{k!}$$

$$P(\text{one or more events in time t}) = 1 - P^*(k=0, t)$$

$$\ln(1-P) = -rt$$

introducing $J_{\text{het}}(T)$, $T(t)$ and INP surface A:

$$\ln\left(1 - P(A,t)\right) = -A \underbrace{\int_0^t J_{\text{het}}(T(t'))\, dt'}_{I(T)}$$

INAS: $$I(T) = n_s(T) = \exp(a \cdot (T - T_{0°C}) + b)$$

Poissonian model of freezing & Ice Nucleation Active Sites (INAS)

theory (in modern notation)
(Bigg '53, Langham & Mason '58, Carte '59, Marshall '61)

Poisson counting process with rate r:

$$P^*(\text{k events in time t}) = \frac{(rt)^k \exp(-rt)}{k!}$$

$$P(\text{one or more events in time t}) = 1 - P^*(k=0,t)$$

$$\ln(1-P) = -rt$$

introducing $J_{\text{het}}(T)$, $T(t)$ and INP surface A:

$$\ln\left(1-P(A,t)\right) = -A \underbrace{\int_0^t J_{\text{het}}(T(t'))\,dt'}_{I(T)}$$

INAS: $I(T) = n_s(T) = \exp(a \cdot (T - T_{0^\circ C}) + b)$

experimental $n_s(T)$ fits: e.g., Niemand et al. 2012

freezing temperature T_{fz} as a super-particle attribute

$$P(A, T_{fz}) = 1 - \exp(-A \cdot n_s(T_{fz}))$$

spectrum of T_{fz} even for monodisperse A

freezing temperature T_{fz} as a super-particle attribute

$$P(A, T_{fz}) = 1 - \exp(-A \cdot n_s(T_{fz}))$$

spectrum of T_{fz} even for monodisperse A

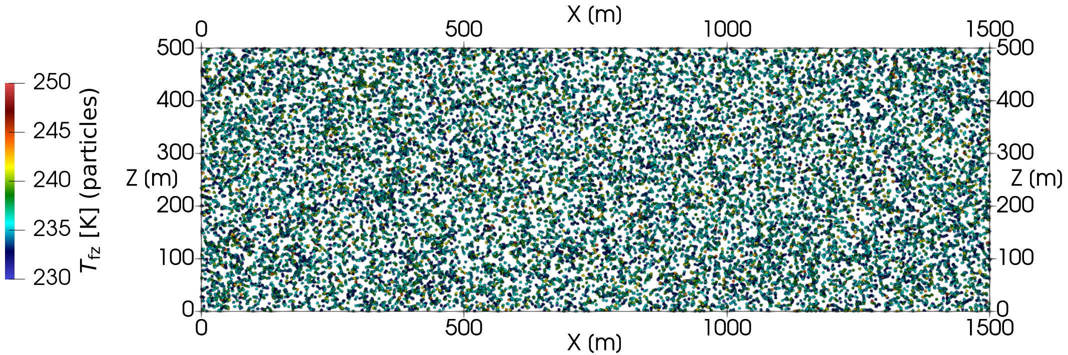

freezing temperature T_{fz} as a super-particle attribute: initialisation

INAS P(T_{fz},A) sampling (A lognormal)

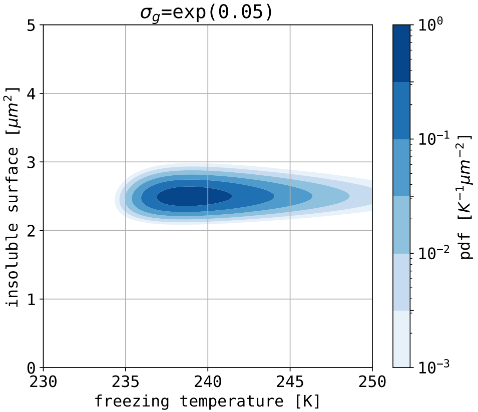

freezing temperature T_{fz} as a super-particle attribute: initialisation

INAS P(T_{fz},A) sampling (A lognormal)

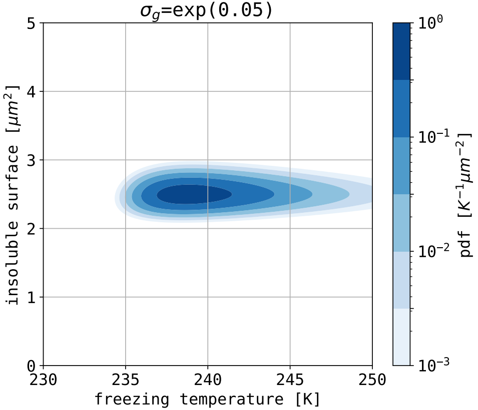

freezing temperature T_{fz} as a super-particle attribute: initialisation

INAS P(T_{fz},A) sampling (A lognormal)

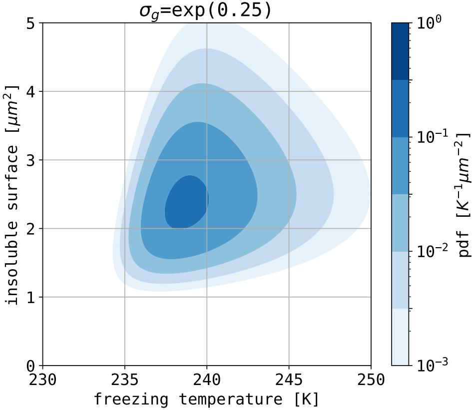

freezing temperature T_{fz} as a super-particle attribute: initialisation

INAS P(T_{fz},A) sampling (A lognormal)

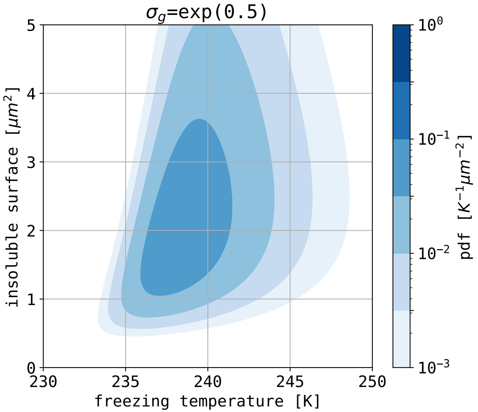

INAS P(T_{fz},A) sampling (A lognormal)

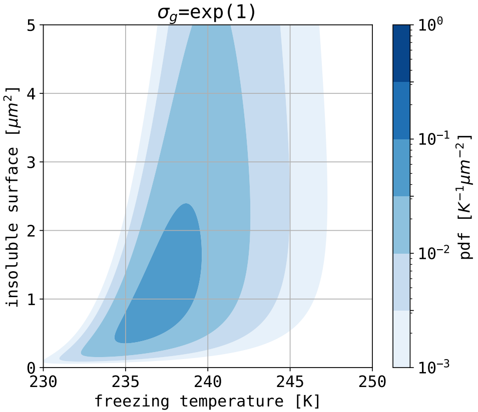

freezing temperature T_{fz} as a super-particle attribute: initialisation

INAS P(T_{fz},A) sampling (A lognormal)

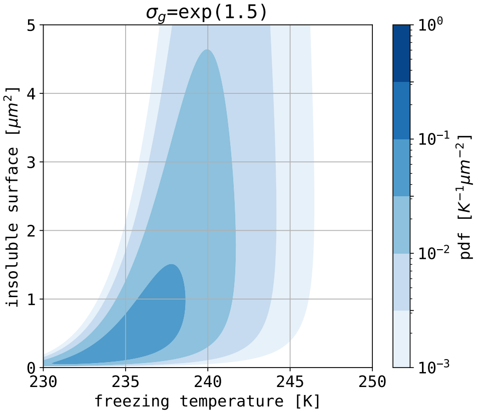

freezing temperature T_{fz} as a super-particle attribute: initialisation

INAS P(T_{fz},A) sampling (A lognormal)

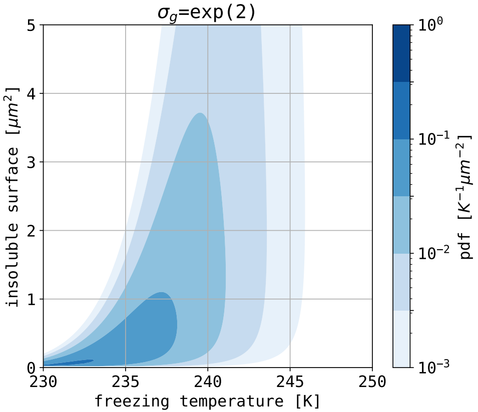

freezing temperature T_{fz} as a super-particle attribute: initialisation

INAS P(T_{fz},A) sampling (A lognormal)

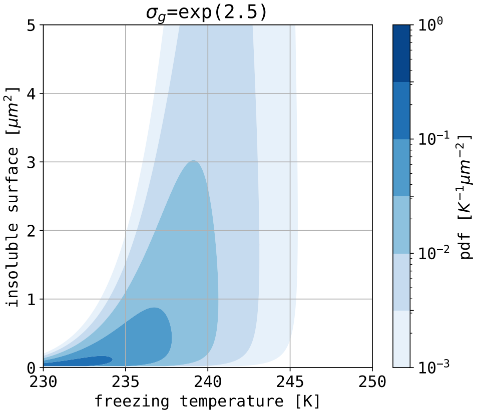

freezing temperature T_{fz} as a super-particle attribute: initialisation

INAS P(T_{fz},A) sampling (A lognormal)

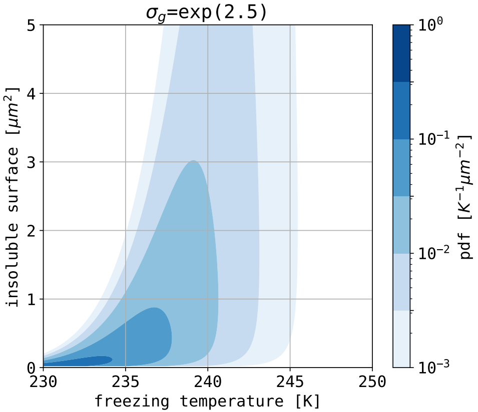

box model (or single grid cell)

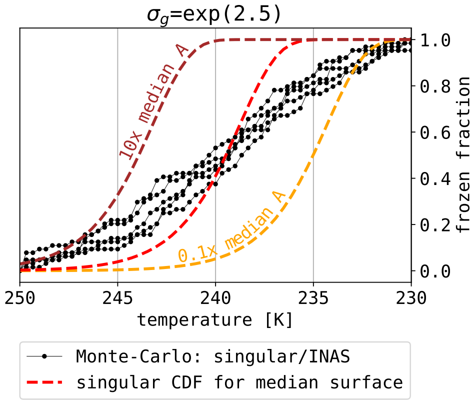

freezing temperature T_{fz} as a super-particle attribute: initialisation

INAS P(T_{fz},A) sampling (A lognormal)

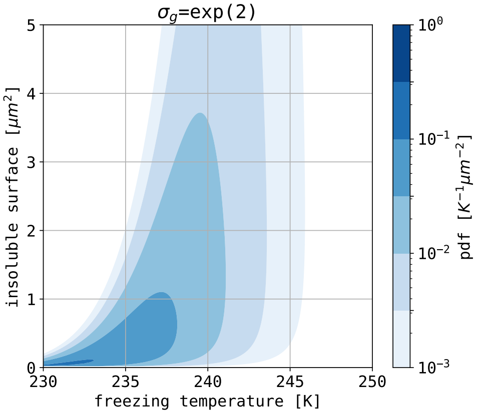

box model (or single grid cell)

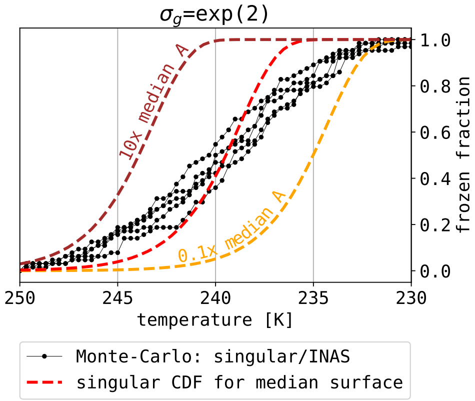

freezing temperature T_{fz} as a super-particle attribute: initialisation

INAS P(T_{fz},A) sampling (A lognormal)

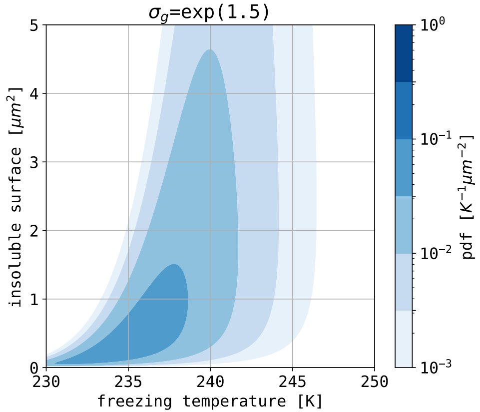

box model (or single grid cell)

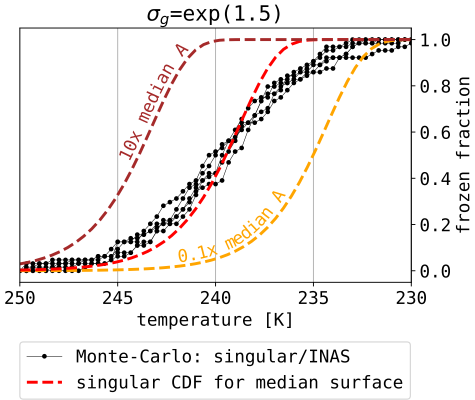

freezing temperature T_{fz} as a super-particle attribute: initialisation

INAS P(T_{fz},A) sampling (A lognormal)

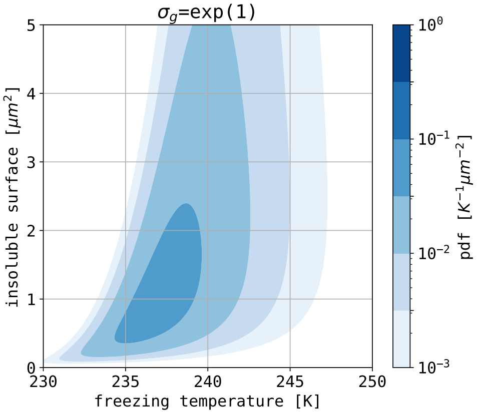

box model (or single grid cell)

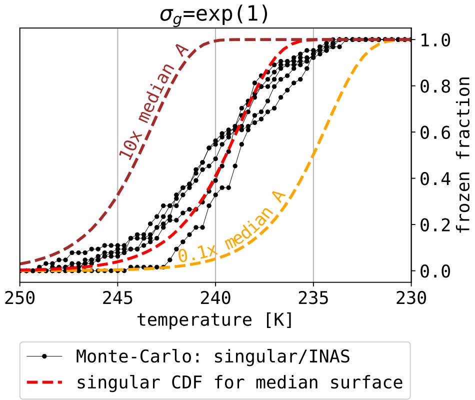

freezing temperature T_{fz} as a super-particle attribute: initialisation

INAS P(T_{fz},A) sampling (A lognormal)

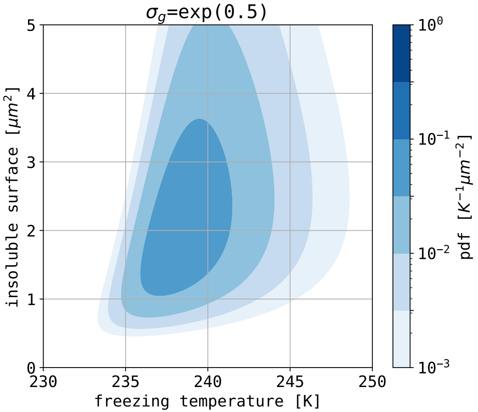

box model (or single grid cell)

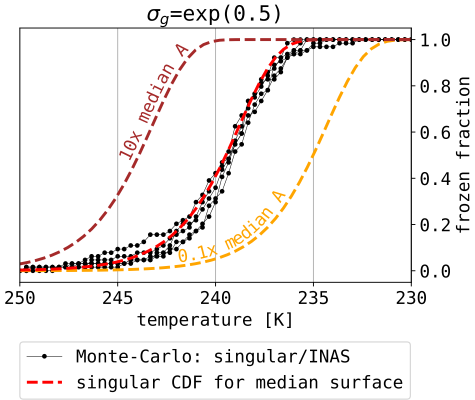

freezing temperature T_{fz} as a super-particle attribute: initialisation

INAS P(T_{fz},A) sampling (A lognormal)

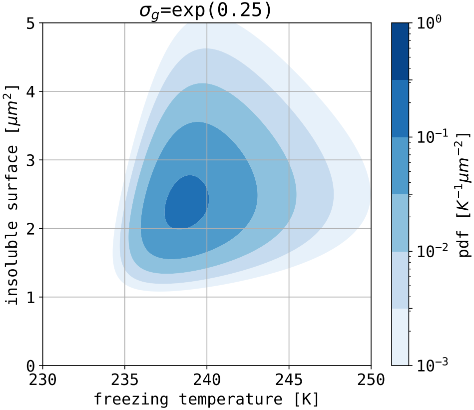

box model (or single grid cell)

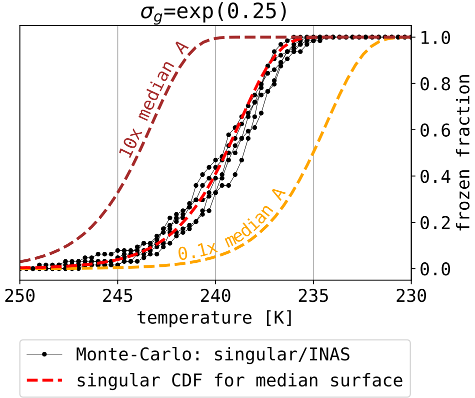

freezing temperature T_{fz} as a super-particle attribute: initialisation

INAS P(T_{fz},A) sampling (A lognormal)

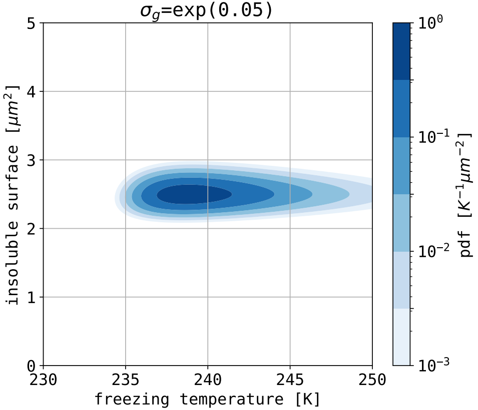

box model (or single grid cell)

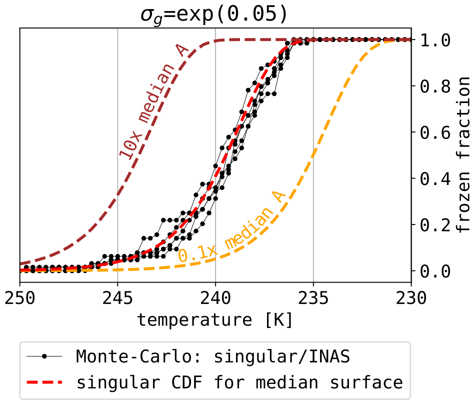

freezing temperature T_{fz} as a super-particle attribute: initialisation

INAS P(T_{fz},A) sampling (A lognormal)

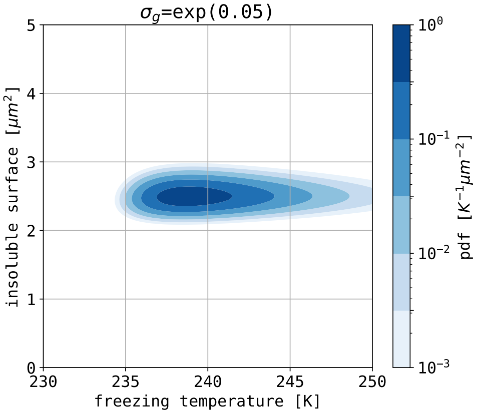

box model (or single grid cell)

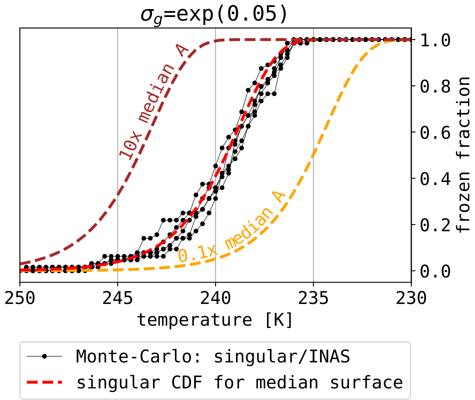

– limitations stemming from monodisperse INP assumption (see also Alpert & Knopf '16)
– singular particle-based model is capable of representing polydisperse INP

particle-based freezing: singular (Shima et al.) / time-dependent (this work)

singular:	INAS T_{fz} **as attribute**; initialisation by random sampling from $P(T_{fz}, A)$ with lognormal A (A is not an attribute, initialisation only); freezing if $T(t) < T_{fz}(t=0)$
time-dependent:	A **as attribute** (randomly sampled from the same lognormal) Monte-Carlo freezing trigger using $P(J_{het}(T(t)))$

particle-based freezing: singular (Shima et al.) / time-dependent (this work)

singular: INAS T_{fz} **as attribute**; initialisation by random sampling from $P(T_{\text{fz}}, A)$ with lognormal A (A is not an attribute, initialisation only); freezing if $T(t) < T_{fz}(t=0)$

time-dependent: A **as attribute** (randomly sampled from the same lognormal)
Monte-Carlo freezing trigger using $P(J_{\text{het}}(T(t)))$

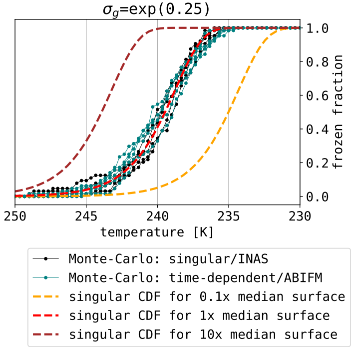

particle-based freezing: singular (Shima et al.) / time-dependent (this work)

singular: INAS T_{fz} **as attribute**; initialisation by random sampling from $P(T_{fz}, A)$ with lognormal A (A is not an attribute, initialisation only); freezing if $T(t) < T_{fz}(t=0)$

time-dependent: A **as attribute** (randomly sampled from the same lognormal)
Monte-Carlo freezing trigger using $P(J_{het}(T(t)))$

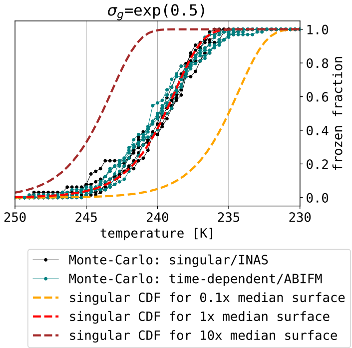

particle-based freezing: singular (Shima et al.) / time-dependent (this work)

singular: INAS T_{fz} **as attribute**; initialisation by random sampling from $P(T_{\mathrm{fz}}, A)$ with lognormal A (A is not an attribute, initialisation only); freezing if $T(t) < T_{fz}(t=0)$

time-dependent: A **as attribute** (randomly sampled from the same lognormal)
Monte-Carlo freezing trigger using $P(J_{\mathrm{het}}(T(t)))$

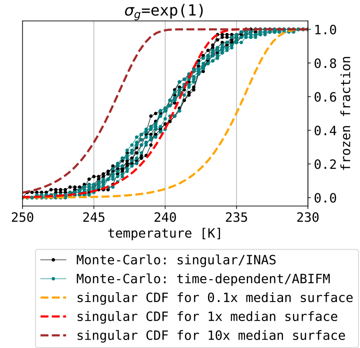

particle-based freezing: singular (Shima et al.) / time-dependent (this work)

singular: INAS T_{fz} **as attribute**; initialisation by random sampling from $P(T_{fz}, A)$ with lognormal A (A is not an attribute, initialisation only); freezing if $T(t) < T_{fz}(t=0)$

time-dependent: A **as attribute** (randomly sampled from the same lognormal) Monte-Carlo freezing trigger using $P(J_{het}(T(t)))$

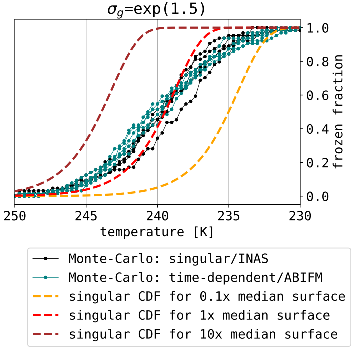

particle-based freezing: singular (Shima et al.) / time-dependent (this work)

singular: INAS T_{fz} **as attribute**; initialisation by random sampling from $P(T_{fz}, A)$ with lognormal A (A is not an attribute, initialisation only); freezing if $T(t) < T_{fz}(t=0)$

time-dependent: A **as attribute** (randomly sampled from the same lognormal)
Monte-Carlo freezing trigger using $P(J_{het}(T(t)))$

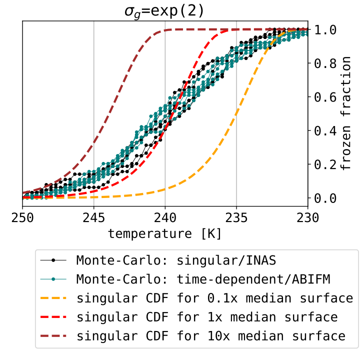

particle-based freezing: singular (Shima et al.) / time-dependent (this work)

singular: INAS T_{fz} **as attribute**; initialisation by random sampling from $P(T_{fz}, A)$ with lognormal A (A is not an attribute, initialisation only); freezing if $T(t) < T_{fz}(t=0)$

time-dependent: A **as attribute** (randomly sampled from the same lognormal) Monte-Carlo freezing trigger using $P(J_{het}(T(t)))$

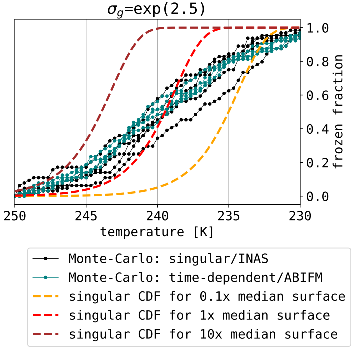

particle-based freezing: singular (Shima et al.) / time-dependent (this work)

singular: INAS T_{fz} **as attribute**; initialisation by random sampling from $P(T_{fz}, A)$ with lognormal A (A is not an attribute, initialisation only); freezing if $T(t) < T_{fz}(t=0)$

time-dependent: A **as attribute** (randomly sampled from the same lognormal) Monte-Carlo freezing trigger using $P(J_{het}(T(t)))$

cooling rate: $0.5\ {}^{K}/_{min}$

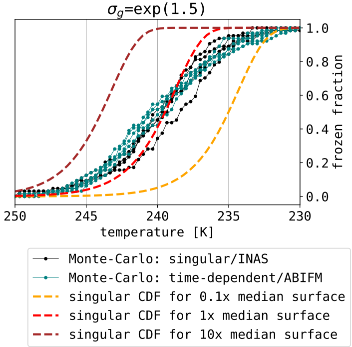

singular: INAS T_{fz} **as attribute**; initialisation by random sampling from $P(T_{\mathrm{fz}}, A)$ with lognormal A (A is not an attribute, initialisation only); freezing if $T(t) < T_{fz}(t=0)$

time-dependent: A **as attribute** (randomly sampled from the same lognormal)
Monte-Carlo freezing trigger using $P(J_{\mathrm{het}}(T(t)))$

cooling rate: 0.1 K/min

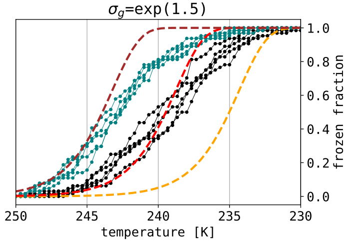

cooling rate: 0.5 K/min

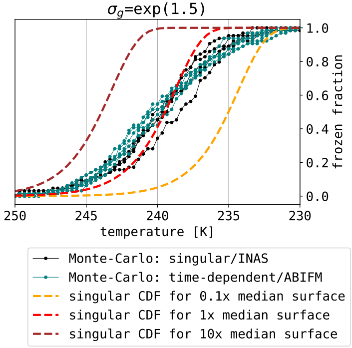

particle-based freezing: singular (Shima et al.) / time-dependent (this work)

singular: INAS T_{fz} **as attribute**; initialisation by random sampling from $P(T_{fz}, A)$ with lognormal A (A is not an attribute, initialisation only); freezing if $T(t) < T_{fz}(t=0)$

time-dependent: A **as attribute** (randomly sampled from the same lognormal) Monte-Carlo freezing trigger using $P(J_{het}(T(t)))$

cooling rate: 0.1 $^K/_{min}$

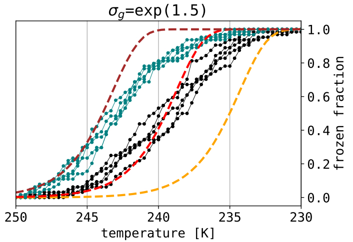

cooling rate: 0.5 $^K/_{min}$

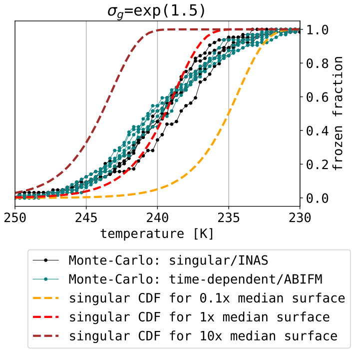

cooling rate: 2.5 $^K/_{min}$

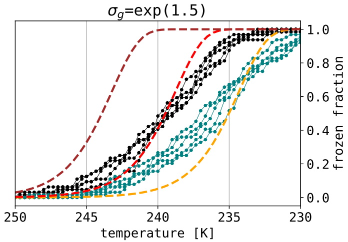

Poissonian model of freezing & Ice Nucleation Active Sites (INAS)

theory (in modern notation)
(Bigg '53, Langham & Mason '58, Carte '59, Marshall '61)

Poisson counting process with rate r:

$$P^*(\text{k events in time t}) = \frac{(rt)^k \exp(-rt)}{k!}$$

$$P(\text{one or more events in time t}) = 1 - P^*(k=0, t)$$

$$\ln(1-P) = -rt$$

introducing $J_{\text{het}}(T)$, $T(t)$ and INP surface A:

$$\ln\left(1-P(A,t)\right) = -A \underbrace{\int_0^t J_{\text{het}}(T(t'))\,dt'}_{I(T)}$$

INAS: $I(T) = n_s(T) = \exp(a \cdot (T - T_{0^\circ C}) + b)$

experimental $n_s(T)$ fits: e.g., Niemand et al. 2012

Poissonian model of freezing & Ice Nucleation Active Sites (INAS)

theory (in modern notation)
(Bigg '53, Langham & Mason '58, Carte '59, Marshall '61)

Poisson counting process with rate r:

$$P^*(\text{k events in time t}) = \frac{(rt)^k \exp(-rt)}{k!}$$

$$P(\text{one or more events in time t}) = 1 - P^*(k=0, t)$$

$$\ln(1-P) = -rt$$

introducing $J_{\text{het}}(T)$, $T(t)$ and INP surface A:

$$\ln\left(1 - P(A,t)\right) = -A \underbrace{\int_0^t J_{\text{het}}(T(t'))\, dt'}_{I(T)}$$

INAS: $I(T) = n_s(T) = \exp(a \cdot (T - T_{0^\circ C}) + b)$

experimental $n_s(T)$ fits: e.g., Niemand et al. 2012

for a constant cooling rate $c = dT/dt$:

$$\ln(1 - P(A,t)) = -\frac{A}{c}\int_{T_0}^{T_0+ct} J_{\text{het}}(T')dT' = -A \cdot I(T)$$

Poissonian model of freezing & Ice Nucleation Active Sites (INAS)

theory (in modern notation)
(Bigg '53, Langham & Mason '58, Carte '59, Marshall '61)

Poisson counting process with rate r:

$$P^*(\text{k events in time t}) = \frac{(rt)^k \exp(-rt)}{k!}$$

$$P(\text{one or more events in time t}) = 1 - P^*(k=0, t)$$

$$\ln(1-P) = -rt$$

introducing $J_{\text{het}}(T)$, $T(t)$ and INP surface A:

$$\ln\left(1-P(A,t)\right) = -A\underbrace{\int_0^t J_{\text{het}}(T(t'))\,dt'}_{I(T)}$$

INAS: $I(T) = n_s(T) = \exp(a\cdot(T - T_{0^\circ C}) + b)$

experimental $n_s(T)$ fits: e.g., Niemand et al. 2012

for a constant cooling rate $c = dT/dt$:

$$\ln(1-P(A,t)) = -\frac{A}{c}\int_{T_0}^{T_0+ct} J_{\text{het}}(T')dT' = -A\cdot I(T)$$

$$\frac{dn_s(T)}{dT} = a\cdot n_s(T) = -\frac{1}{c}J_{\text{het}}(T)$$

Poissonian model of freezing & Ice Nucleation Active Sites (INAS)

theory (in modern notation)
(Bigg '53, Langham & Mason '58, Carte '59, Marshall '61)

Poisson counting process with rate r:

$$P^*(\text{k events in time t}) = \frac{(rt)^k \exp(-rt)}{k!}$$

$$P(\text{one or more events in time t}) = 1 - P^*(k=0, t)$$

$$\ln(1-P) = -rt$$

introducing $J_{\text{het}}(T)$, $T(t)$ and INP surface A:

$$\ln\left(1 - P(A,t)\right) = -A \underbrace{\int_0^t J_{\text{het}}(T(t'))\, dt'}_{I(T)}$$

INAS: $I(T) = n_s(T) = \exp(a \cdot (T - T_{0^\circ C}) + b)$

experimental $n_s(T)$ fits: e.g., Niemand et al. 2012

for a constant cooling rate $c = dT/dt$:

$$\ln(1 - P(A,t)) = -\frac{A}{c}\int_{T_0}^{T_0+ct} J_{\text{het}}(T')dT' = -A \cdot I(T)$$

$$\frac{dn_s(T)}{dT} = a \cdot n_s(T) = -\frac{1}{c} J_{\text{het}}(T)$$

experimental fits: INAS n_s (Niemand et al. '12)
ABIFM J_{het} (Knopf & Alpert '13)

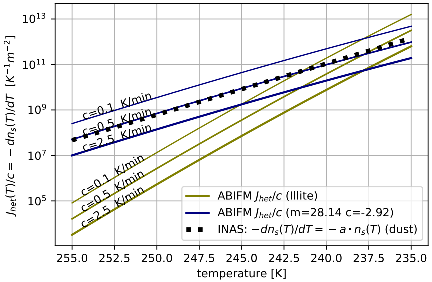

Poissonian model of freezing & Ice Nucleation Active Sites (INAS)

Houston, we have a problem

for a constant cooling rate $c = dT/dt$:

$$\ln(1 - P(A, t)) = -\frac{A}{c}\int_{T_0}^{T_0+ct} J_{\mathrm{het}}(T')dT' = -A \cdot I(T)$$

$$\frac{dn_s(T)}{dT} = a \cdot n_s(T) = -\frac{1}{c}J_{\mathrm{het}}(T)$$

experimental fits: INAS n_s (Niemand et al. '12)
ABIFM J_{het} (Knopf & Alpert '13)

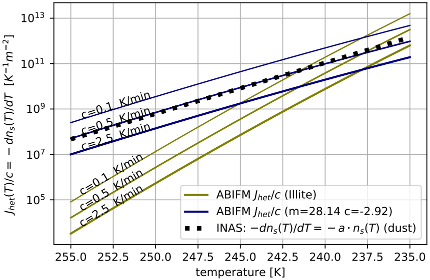

addressed in the modified singular model of Vali '94 (also: Murray et al. '11)
but the singular ansatz limitation of sampling T_{fz} at t=0 remains

particle-based μ-physics + prescribed-flow test (aka KiD-2D)[a,b,c,d,e]

Lagrangian component (PySDM)

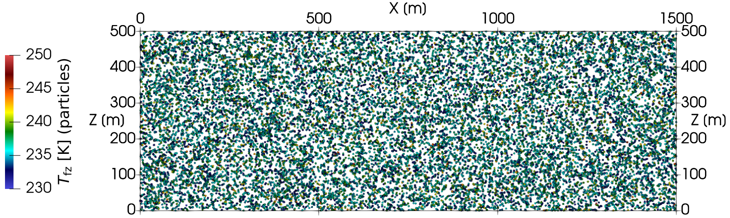

Eulerian component (PyMPDATA)

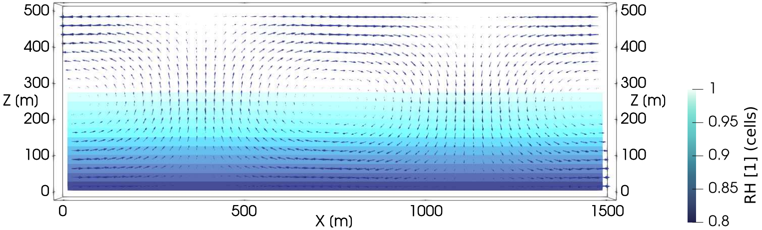

[a] concept: Gedzelman & Arnold '93
[b] stratiform: Morrison & Grabowski '07
[c] particle-based: Arabas et al. '15
[d] KiD-2D: github.com/BShipway/KiD
[e] here: SHEBA case (Fridlind et al. '12)

particle-based μ-physics + prescribed-flow test (aka KiD-2D)[a,b,c,d,e]

Lagrangian component (PySDM)

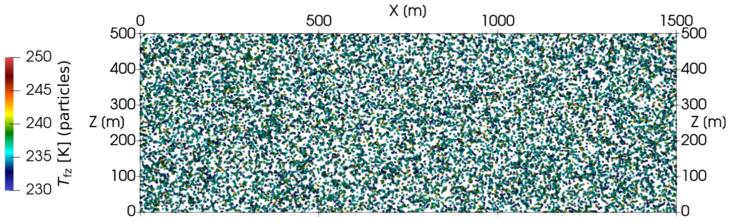

Eulerian component (PyMPDATA)

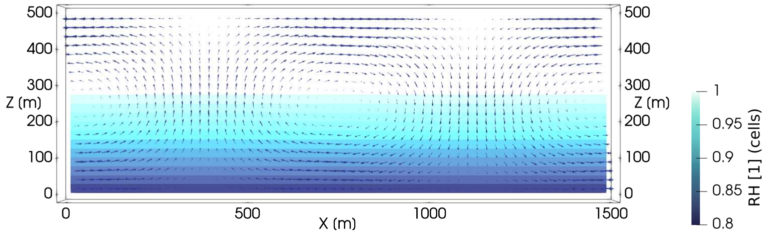

PySDM & PyMPDATA
(Bartman et al. 2022)

- new packages
  (pip install PySDM PyMPDATA)
- open-source
  github.com/atmos-cloud-sim-uj
- pure Python, multi-threaded
  (Numba/LLVM JIT)
- Jupyter & Colab friendly
  single-click reproducible in the cloud

[a] concept: Gedzelman & Arnold '93
[b] stratiform: Morrison & Grabowski '07
[c] particle-based: Arabas et al. '15
[d] KiD-2D: github.com/BShipway/KiD
[e] here: SHEBA case (Fridlind et al. '12)

particle-based μ-physics + prescribed-flow test

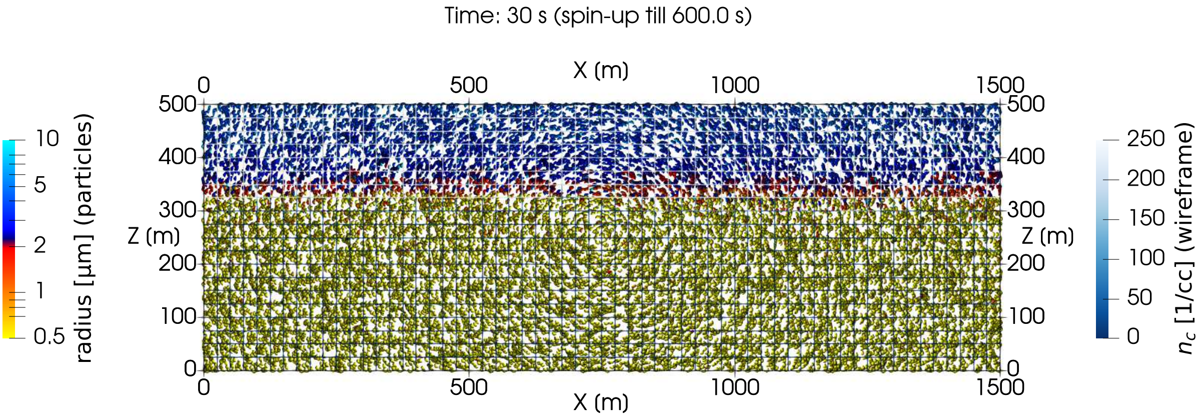

16+16 super-particles/cell for INP-rich + INP-free particles

$N_{\text{aer}} = 300/cc$ (two-mode lognormal) $N_{\text{INP}} = 150/L$ (lognormal, $D_g = 0.74\ \mu$m, $\sigma_g = 2.55$)

particle-based μ-physics + prescribed-flow test

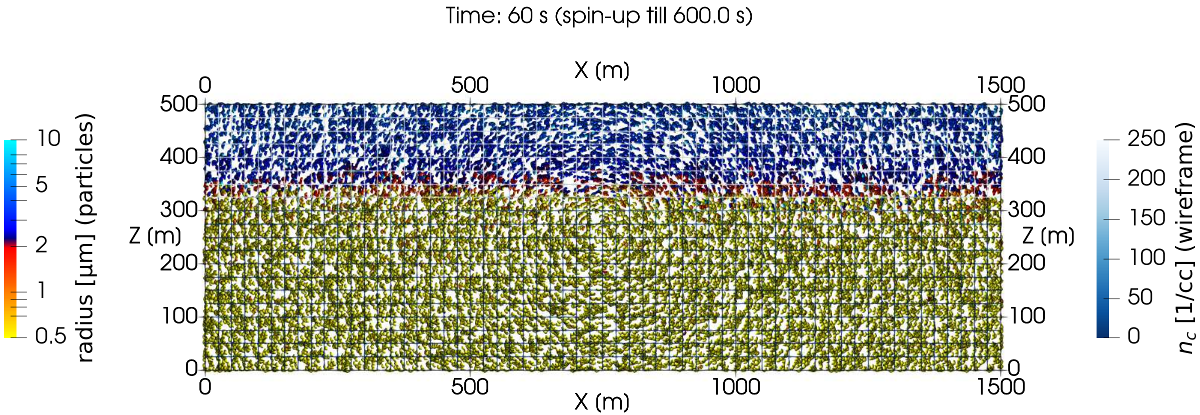

16+16 super-particles/cell for INP-rich + INP-free particles

$N_{\text{aer}} = 300/cc$ (two-mode lognormal) $N_{\text{INP}} = 150/L$ (lognormal, $D_g = 0.74\ \mu\text{m}$, $\sigma_g = 2.55$)

particle-based μ-physics + prescribed-flow test

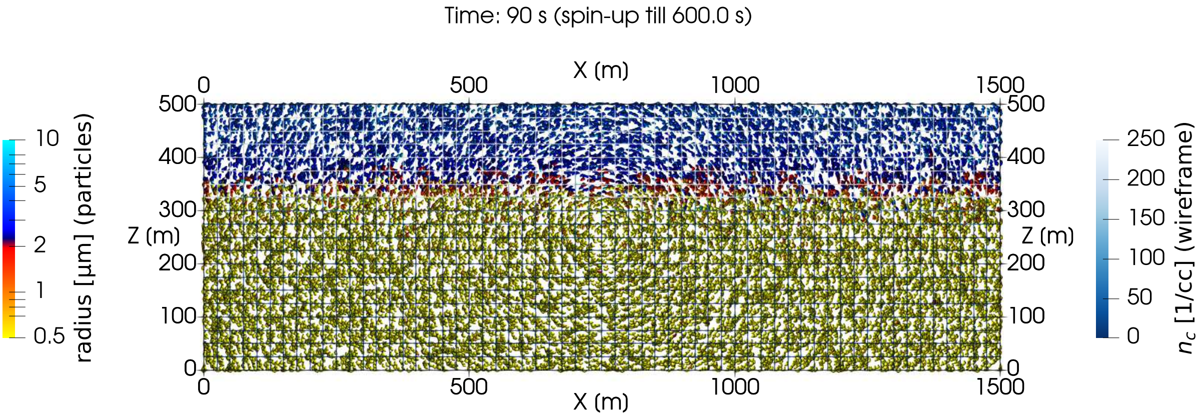

16+16 super-particles/cell for INP-rich + INP-free particles

$N_{\text{aer}} = 300/cc$ (two-mode lognormal) $N_{\text{INP}} = 150/L$ (lognormal, $D_g = 0.74\ \mu\text{m}$, $\sigma_g = 2.55$)

particle-based μ-physics + prescribed-flow test

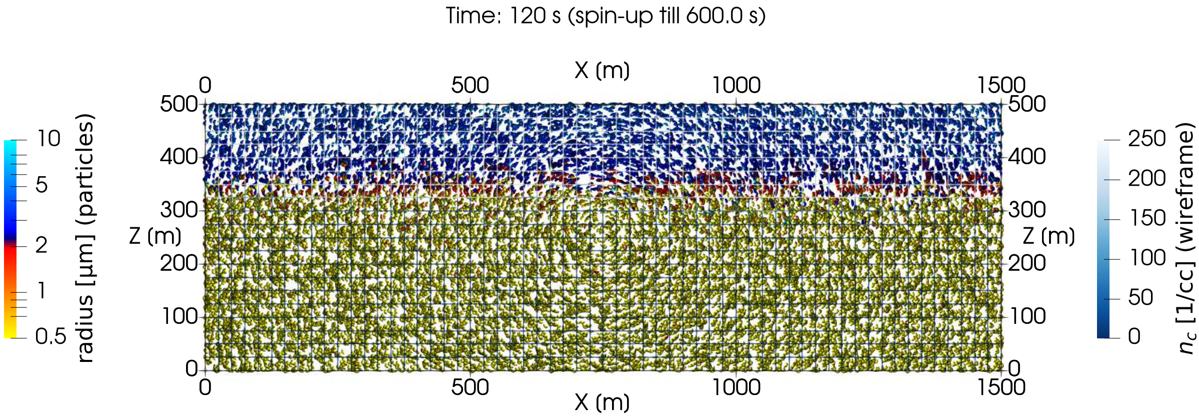

16+16 super-particles/cell for INP-rich + INP-free particles

$N_{\text{aer}} = 300/cc$ (two-mode lognormal) $N_{\text{INP}} = 150/L$ (lognormal, $D_g = 0.74\ \mu$m, $\sigma_g = 2.55$)

particle-based μ-physics + prescribed-flow test

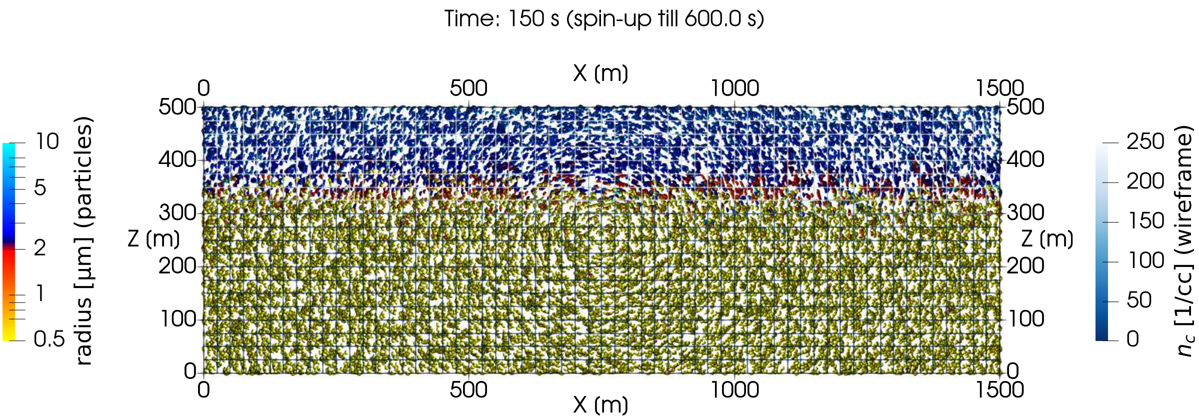

16+16 super-particles/cell for INP-rich + INP-free particles

N_{aer} = 300/*cc* (two-mode lognormal) N_{INP} = 150/*L* (lognormal, D_g=0.74 μm, σ_g=2.55)

particle-based μ-physics + prescribed-flow test

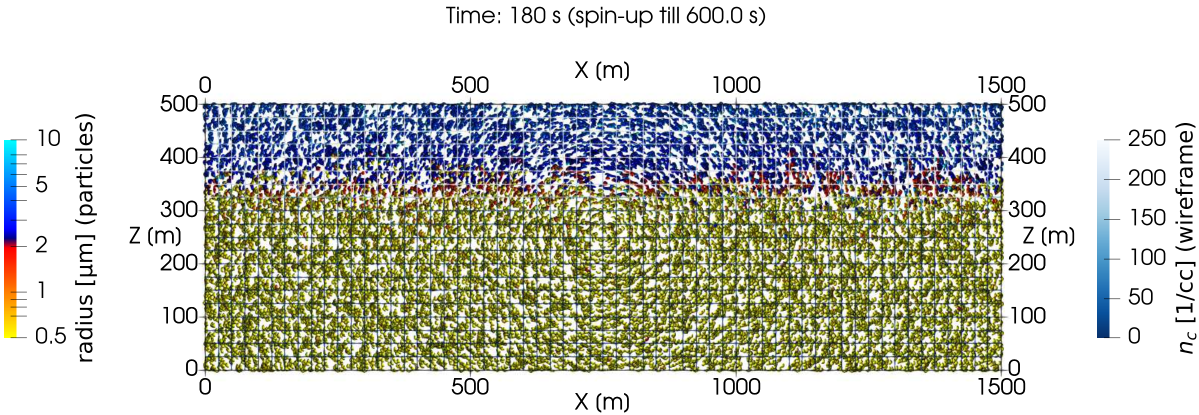

16+16 super-particles/cell for INP-rich + INP-free particles

$N_{\text{aer}} = 300/cc$ (two-mode lognormal) $N_{\text{INP}} = 150/L$ (lognormal, $D_g = 0.74\ \mu$m, $\sigma_g = 2.55$)

particle-based μ-physics + prescribed-flow test

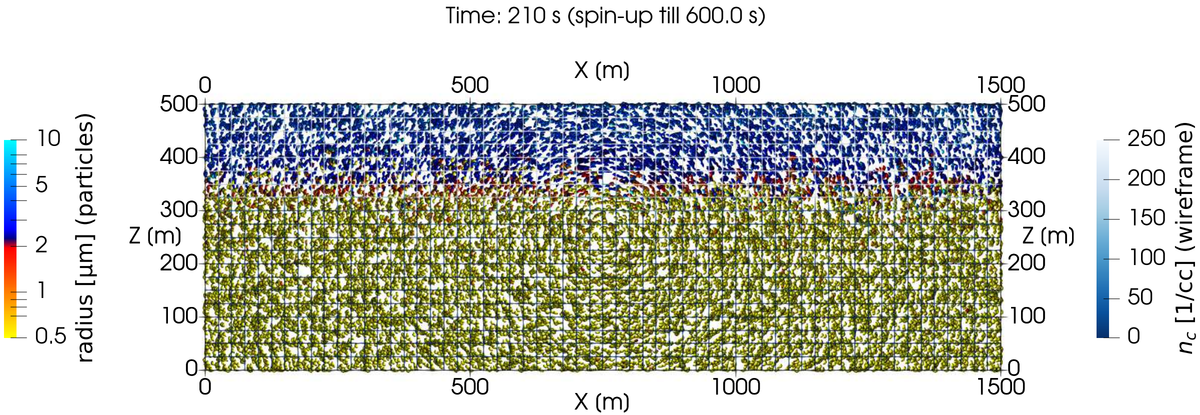

16+16 super-particles/cell for INP-rich + INP-free particles

$N_{aer} = 300/cc$ (two-mode lognormal) $N_{INP} = 150/L$ (lognormal, $D_g = 0.74\ \mu m$, $\sigma_g = 2.55$)

particle-based μ-physics + prescribed-flow test

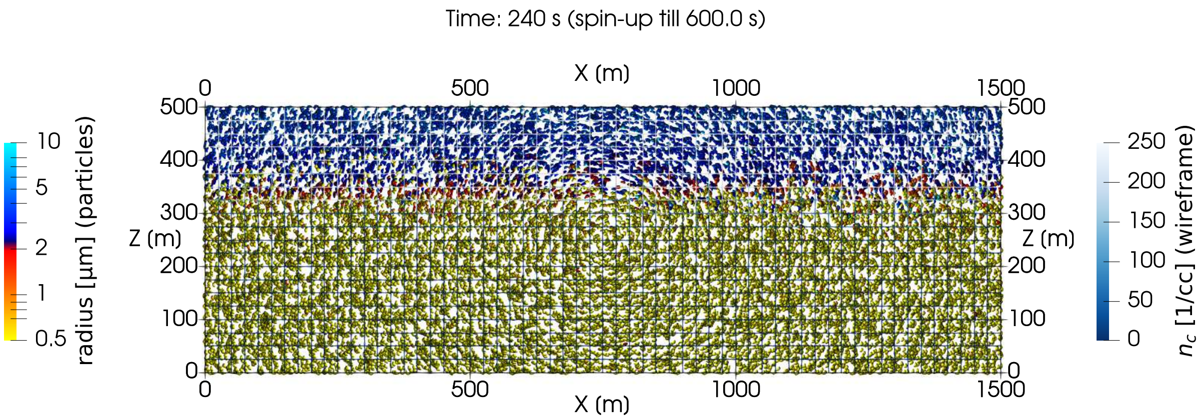

16+16 super-particles/cell for INP-rich + INP-free particles

$N_{aer} = 300/cc$ (two-mode lognormal) $N_{INP} = 150/L$ (lognormal, $D_g = 0.74\ \mu m$, $\sigma_g = 2.55$)

particle-based μ-physics + prescribed-flow test

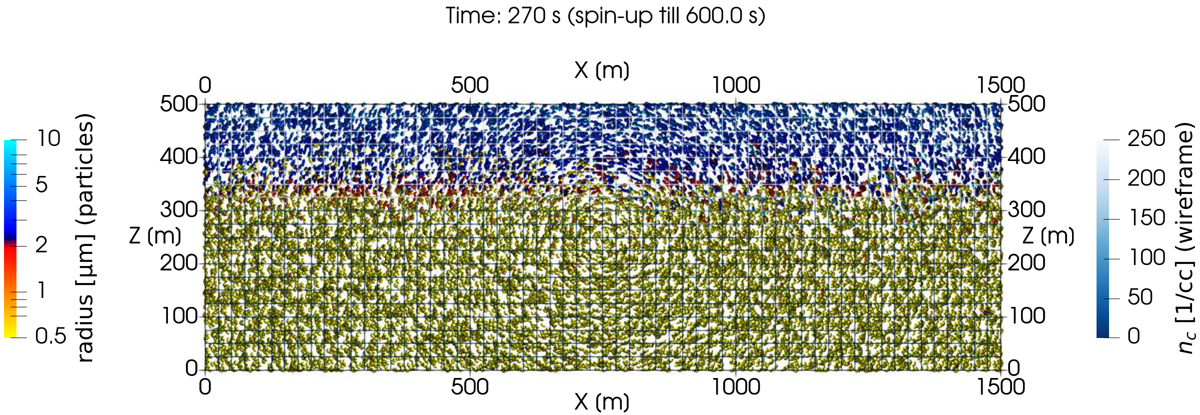

16+16 super-particles/cell for INP-rich + INP-free particles
$N_{aer} = 300/cc$ (two-mode lognormal) $N_{INP} = 150/L$ (lognormal, $D_g = 0.74\ \mu m$, $\sigma_g = 2.55$)

particle-based μ-physics + prescribed-flow test

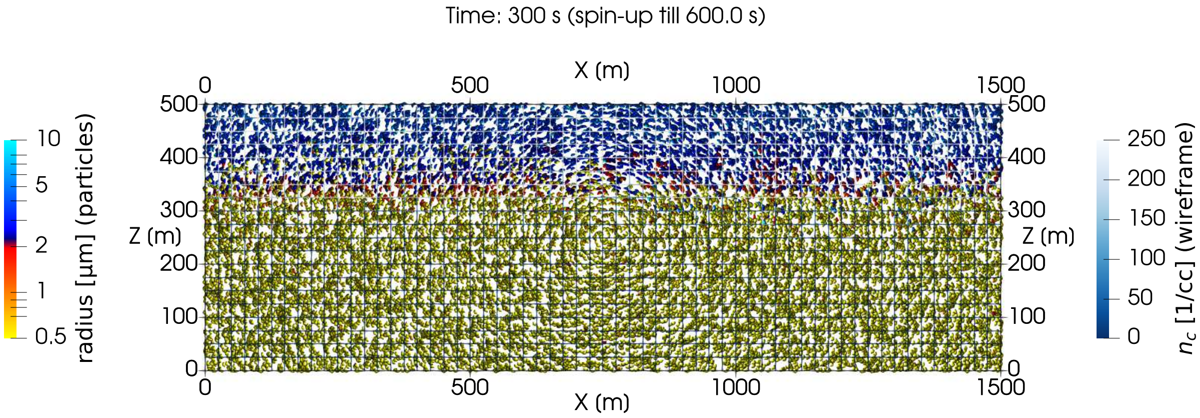

16+16 super-particles/cell for INP-rich + INP-free particles

$N_{\text{aer}} = 300/cc$ (two-mode lognormal) $N_{\text{INP}} = 150/L$ (lognormal, $D_g = 0.74\ \mu\text{m}$, $\sigma_g = 2.55$)

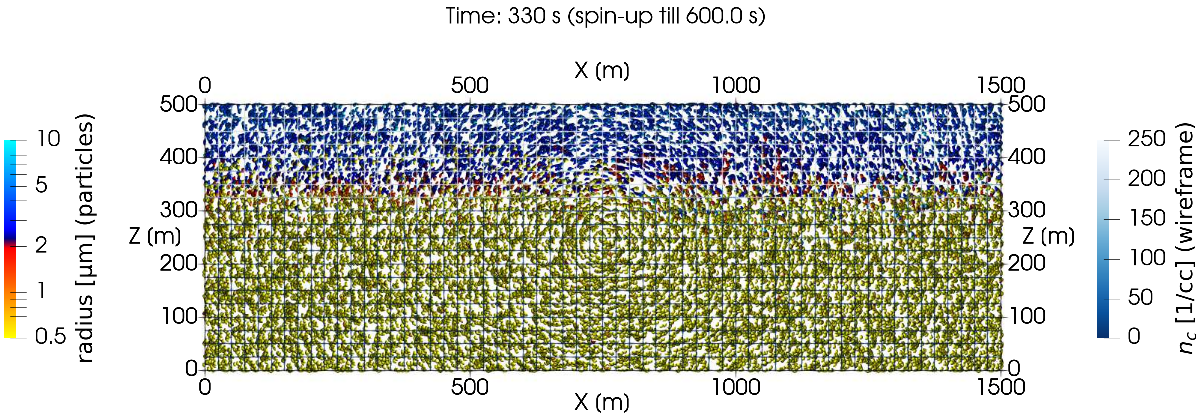

16+16 super-particles/cell for INP-rich + INP-free particles

$N_{\text{aer}} = 300/cc$ (two-mode lognormal) $N_{\text{INP}} = 150/L$ (lognormal, $D_g = 0.74\ \mu$m, $\sigma_g = 2.55$)

particle-based μ-physics + prescribed-flow test

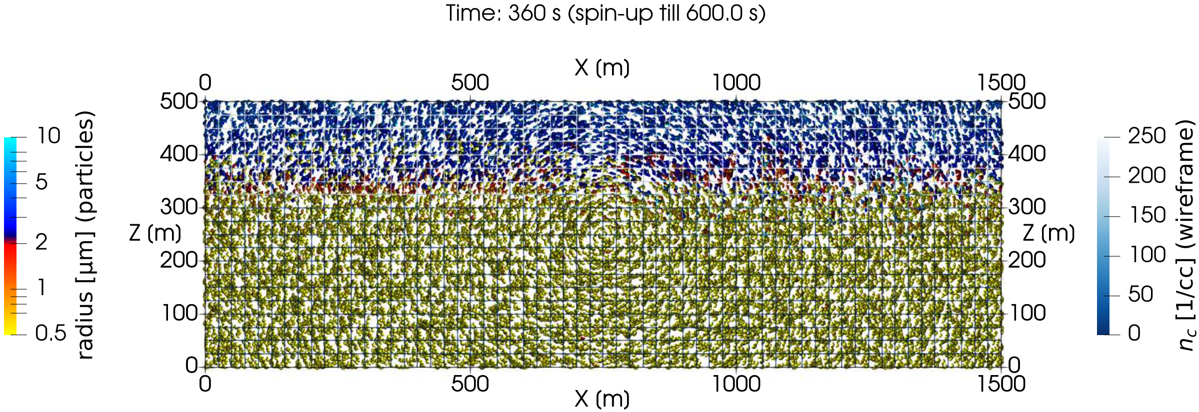

16+16 super-particles/cell for INP-rich + INP-free particles

$N_{\text{aer}} = 300/cc$ (two-mode lognormal) $N_{\text{INP}} = 150/L$ (lognormal, $D_g = 0.74$ μm, $\sigma_g = 2.55$)

particle-based μ-physics + prescribed-flow test

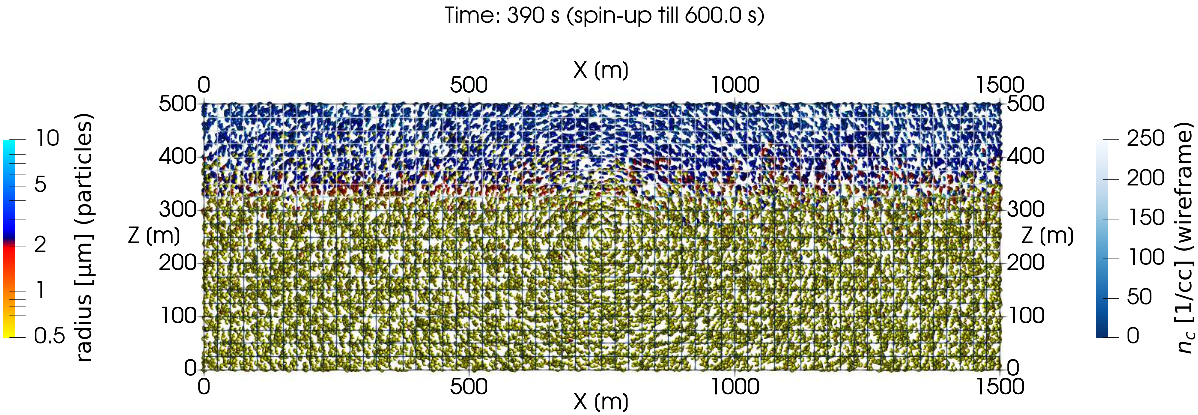

16+16 super-particles/cell for INP-rich + INP-free particles

$N_{\text{aer}} = 300/cc$ (two-mode lognormal) $N_{\text{INP}} = 150/L$ (lognormal, $D_g = 0.74\ \mu$m, $\sigma_g = 2.55$)

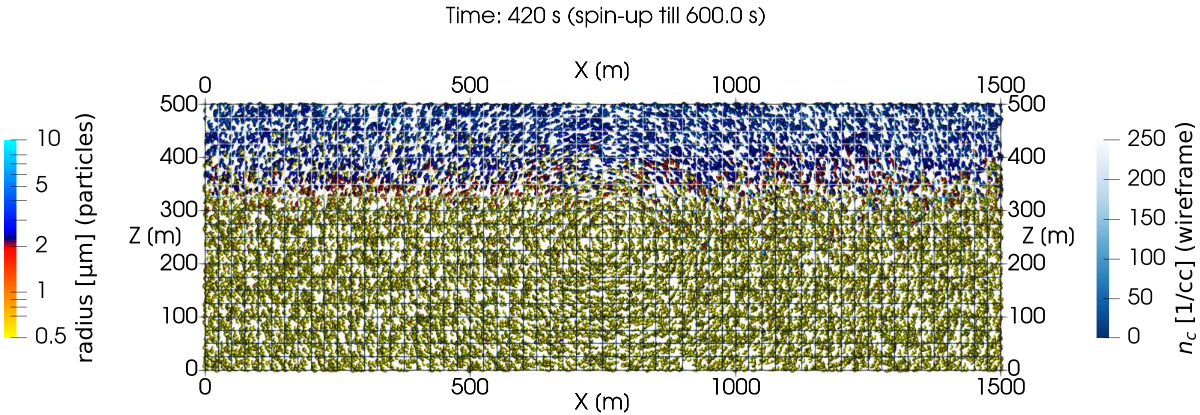

16+16 super-particles/cell for INP-rich + INP-free particles

$N_{\text{aer}} = 300/cc$ (two-mode lognormal) $N_{\text{INP}} = 150/L$ (lognormal, $D_g = 0.74\ \mu\text{m}$, $\sigma_g = 2.55$)

particle-based μ-physics + prescribed-flow test

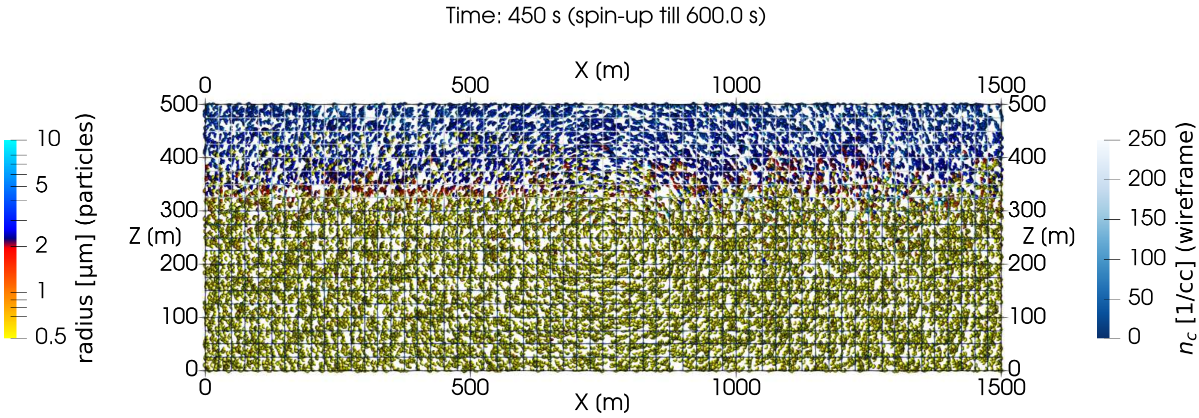

16+16 super-particles/cell for INP-rich + INP-free particles

$N_{\text{aer}} = 300/cc$ (two-mode lognormal) $N_{\text{INP}} = 150/L$ (lognormal, $D_g = 0.74\ \mu$m, $\sigma_g = 2.55$)

particle-based μ-physics + prescribed-flow test

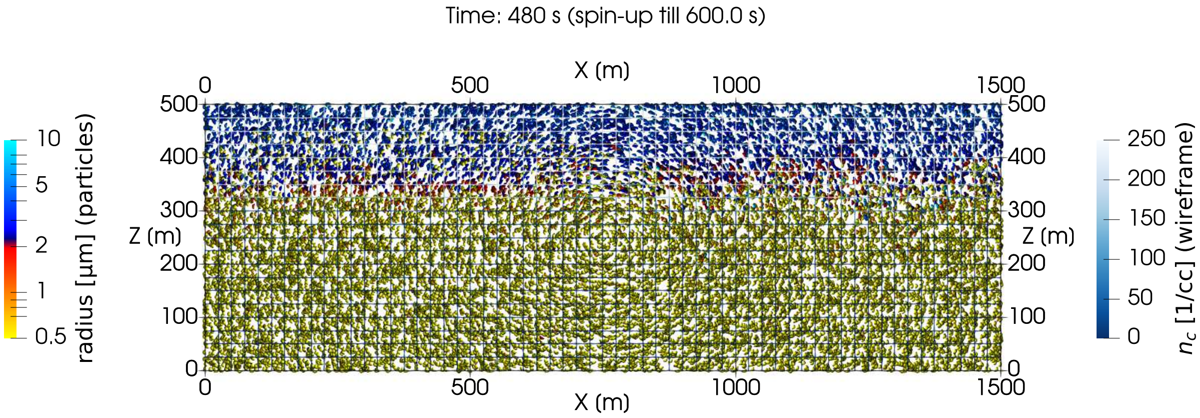

16+16 super-particles/cell for INP-rich + INP-free particles

$N_{\text{aer}} = 300/cc$ (two-mode lognormal) $N_{\text{INP}} = 150/L$ (lognormal, $D_g = 0.74\ \mu$m, $\sigma_g = 2.55$)

particle-based μ-physics + prescribed-flow test

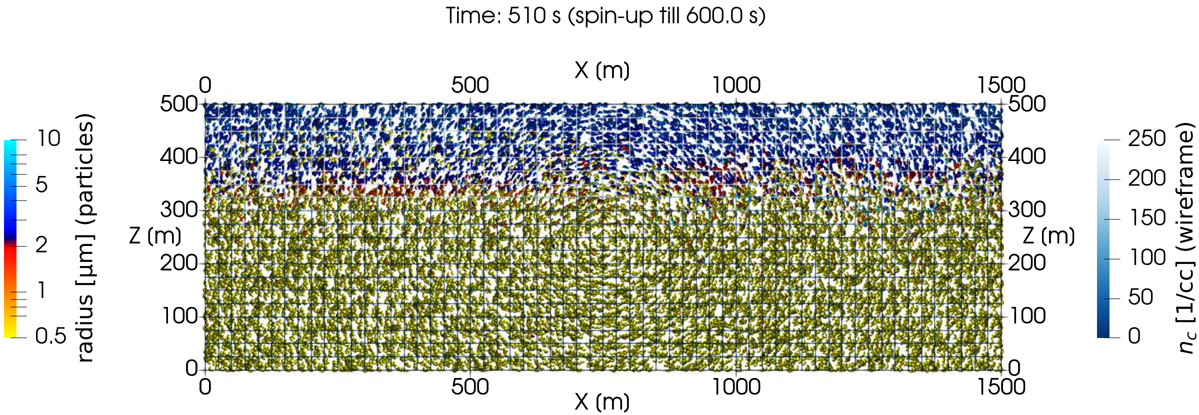

16+16 super-particles/cell for INP-rich + INP-free particles

$N_{\text{aer}} = 300/cc$ (two-mode lognormal) $N_{\text{INP}} = 150/L$ (lognormal, $D_g = 0.74$ μm, $\sigma_g = 2.55$)

particle-based μ-physics + prescribed-flow test

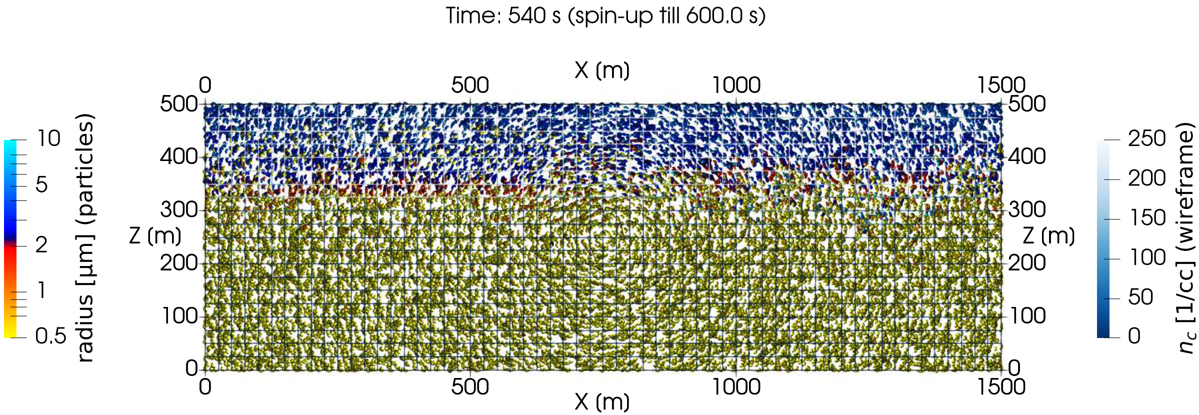

16+16 super-particles/cell for INP-rich + INP-free particles

$N_{aer} = 300/cc$ (two-mode lognormal) $N_{INP} = 150/L$ (lognormal, $D_g = 0.74$ μm, $\sigma_g = 2.55$)

particle-based μ-physics + prescribed-flow test

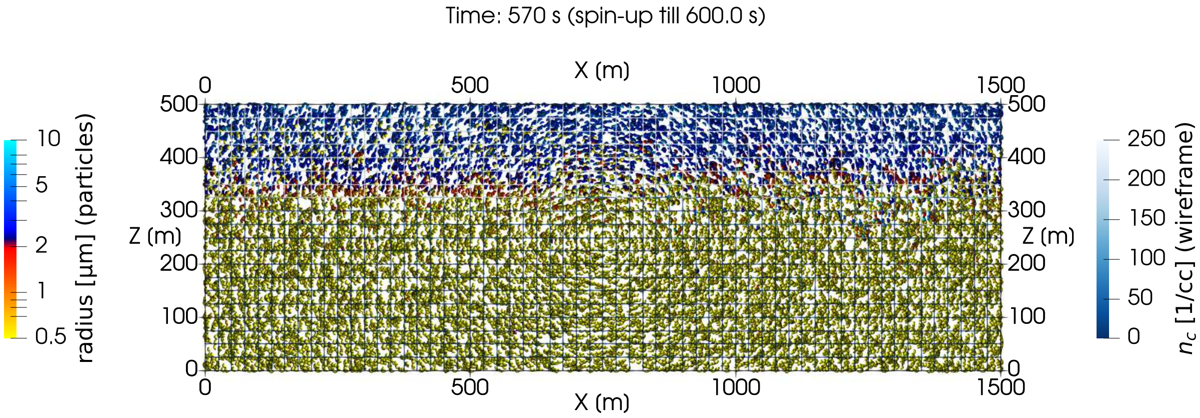

16+16 super-particles/cell for INP-rich + INP-free particles

$N_{aer} = 300/cc$ (two-mode lognormal) $N_{INP} = 150/L$ (lognormal, $D_g = 0.74\ \mu m$, $\sigma_g = 2.55$)

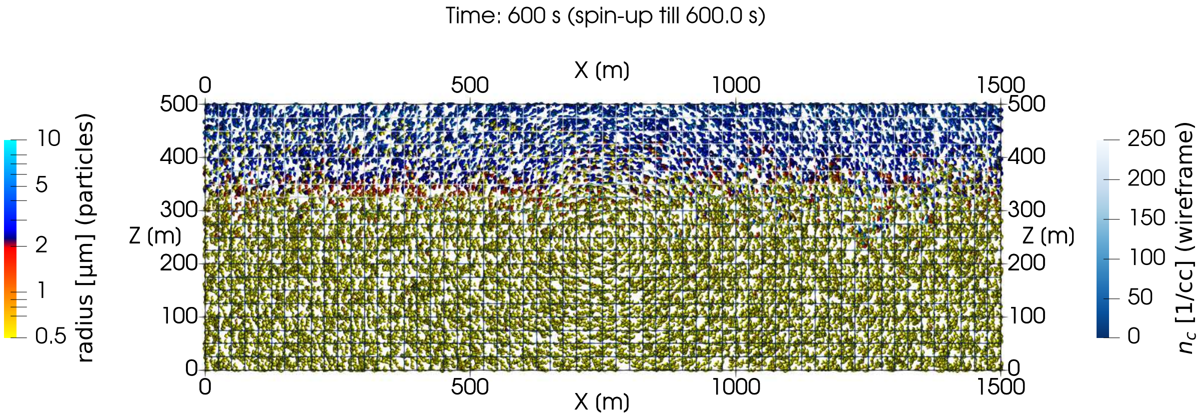

16+16 super-particles/cell for INP-rich + INP-free particles

$N_{\text{aer}} = 300/cc$ (two-mode lognormal) $N_{\text{INP}} = 150/L$ (lognormal, $D_g = 0.74\ \mu\text{m}$, $\sigma_g = 2.55$)

particle-based μ-physics + prescribed-flow test

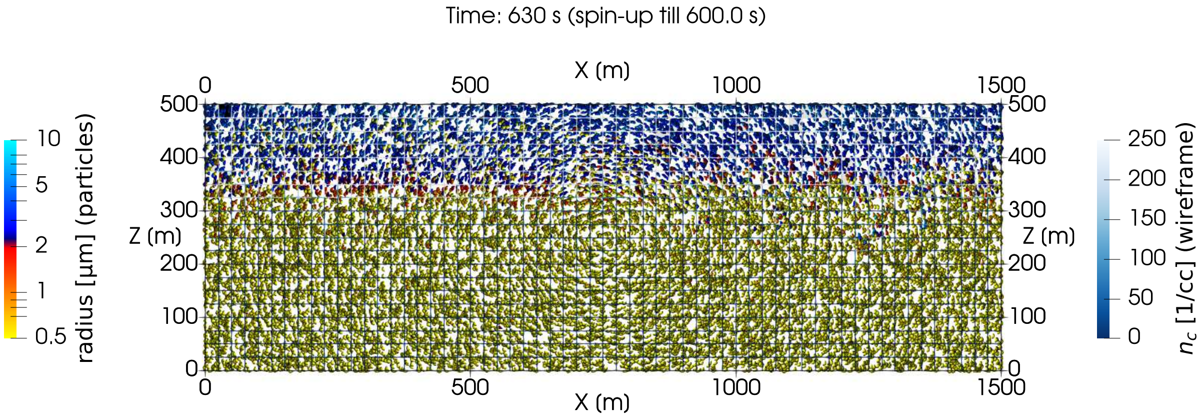

16+16 super-particles/cell for INP-rich + INP-free particles

$N_{\text{aer}} = 300/cc$ (two-mode lognormal) $N_{\text{INP}} = 150/L$ (lognormal, $D_g = 0.74\ \mu$m, $\sigma_g = 2.55$)

particle-based μ-physics + prescribed-flow test

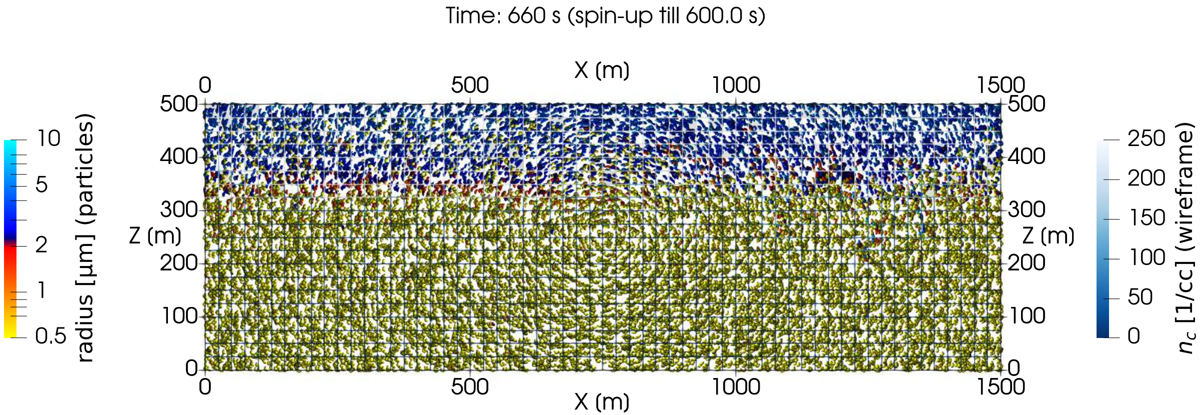

16+16 super-particles/cell for INP-rich + INP-free particles

$N_{\text{aer}} = 300/cc$ (two-mode lognormal) $N_{\text{INP}} = 150/L$ (lognormal, $D_g = 0.74\ \mu\text{m}$, $\sigma_g = 2.55$)

particle-based μ-physics + prescribed-flow test

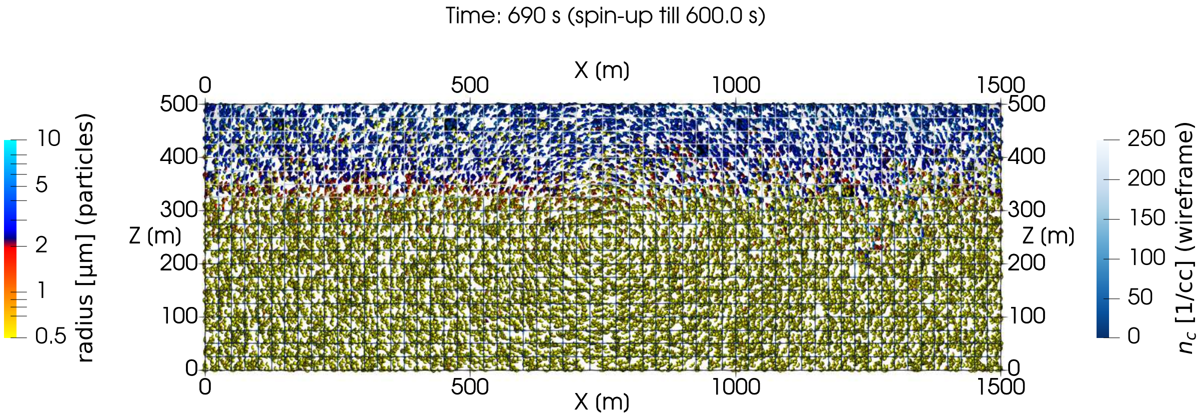

16+16 super-particles/cell for INP-rich + INP-free particles

$N_{\text{aer}} = 300/cc$ (two-mode lognormal) $N_{\text{INP}} = 150/L$ (lognormal, $D_g = 0.74\ \mu$m, $\sigma_g = 2.55$)

particle-based μ-physics + prescribed-flow test

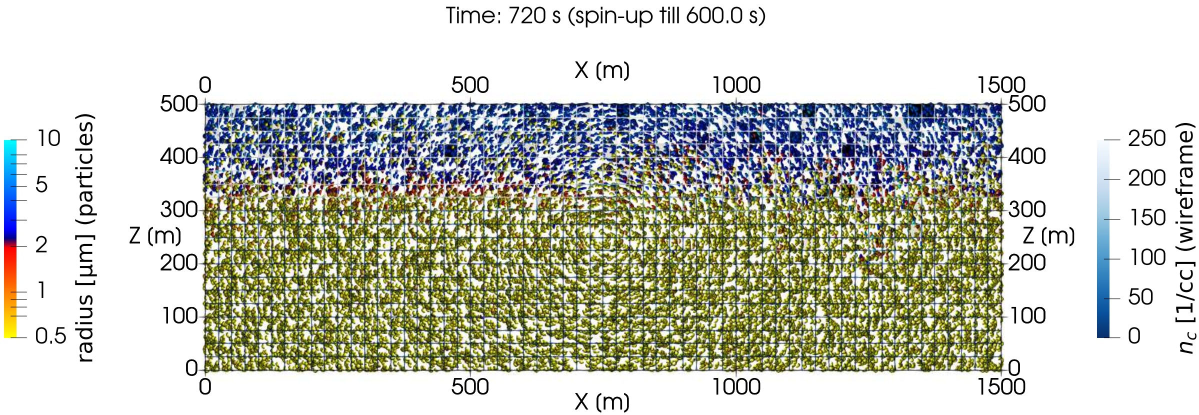

16+16 super-particles/cell for INP-rich + INP-free particles

$N_{\text{aer}} = 300/cc$ (two-mode lognormal) $N_{\text{INP}} = 150/L$ (lognormal, $D_g = 0.74\ \mu$m, $\sigma_g = 2.55$)

particle-based μ-physics + prescribed-flow test

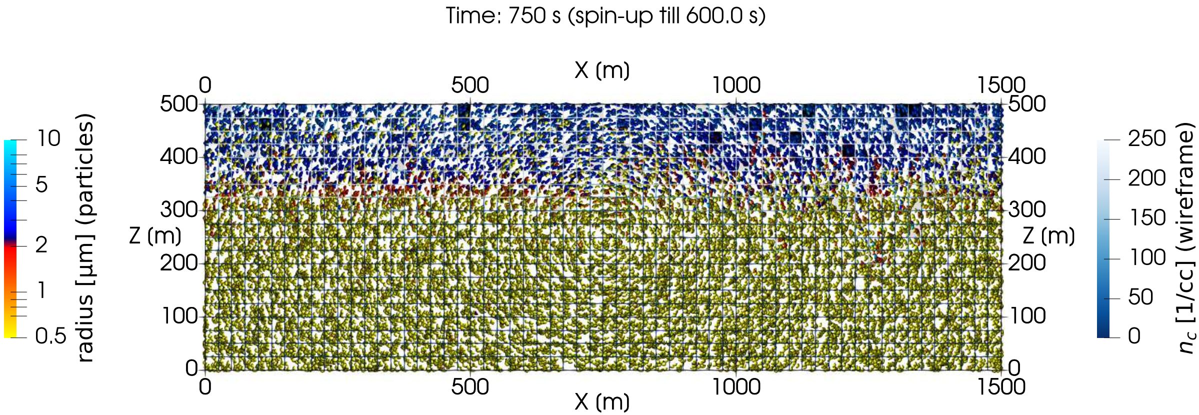

16+16 super-particles/cell for INP-rich + INP-free particles

$N_{aer} = 300/cc$ (two-mode lognormal) $N_{INP} = 150/L$ (lognormal, $D_g = 0.74$ μm, $\sigma_g = 2.55$)

particle-based μ-physics + prescribed-flow test

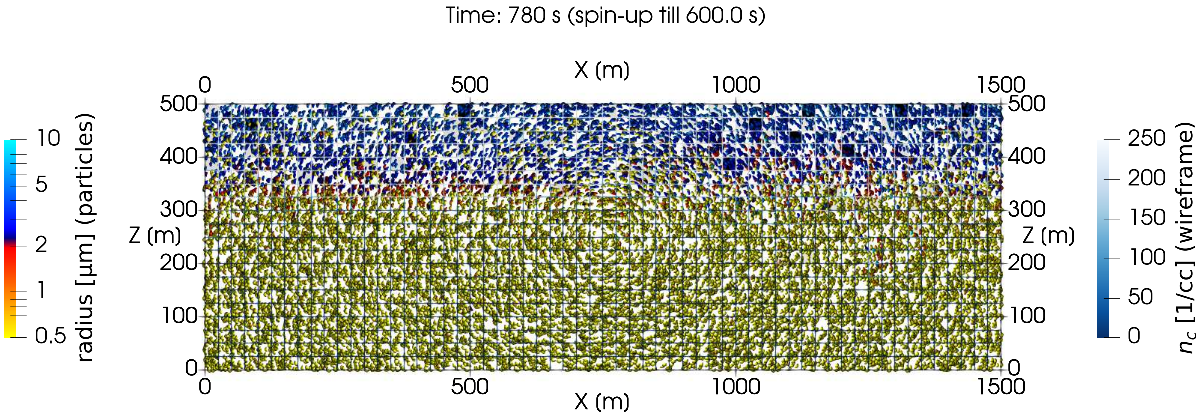

16+16 super-particles/cell for INP-rich + INP-free particles

$N_{\text{aer}} = 300/cc$ (two-mode lognormal) $N_{\text{INP}} = 150/L$ (lognormal, $D_g = 0.74\ \mu$m, $\sigma_g = 2.55$)

particle-based μ-physics + prescribed-flow test

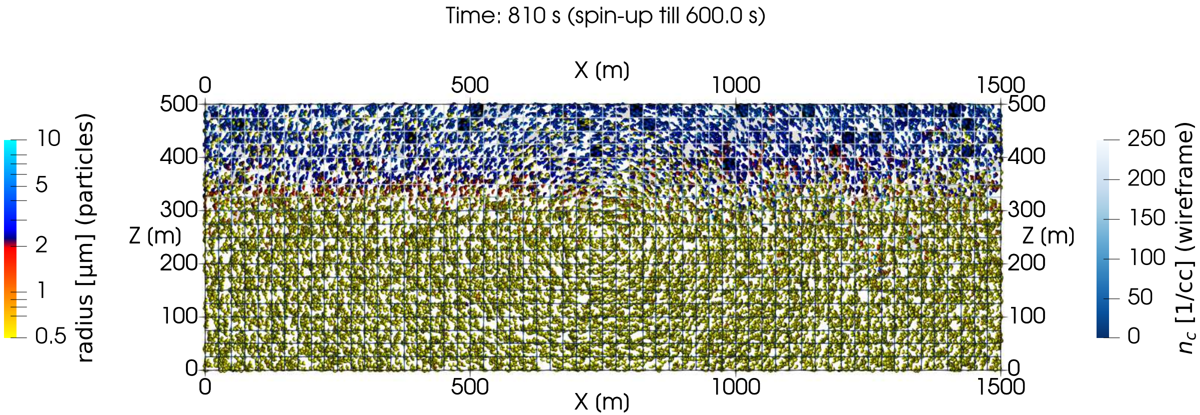

16+16 super-particles/cell for INP-rich + INP-free particles

$N_{\text{aer}} = 300/cc$ (two-mode lognormal) $N_{\text{INP}} = 150/L$ (lognormal, $D_g = 0.74\ \mu$m, $\sigma_g = 2.55$)

particle-based μ-physics + prescribed-flow test

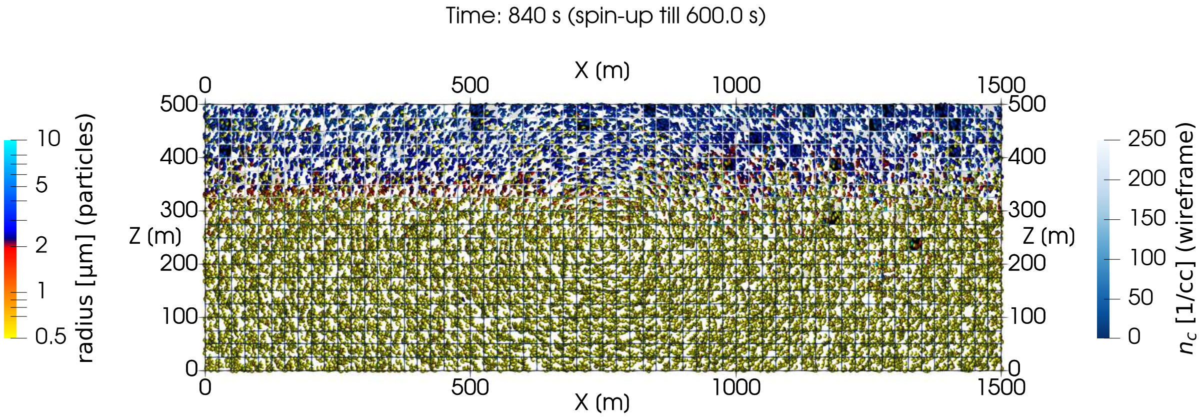

16+16 super-particles/cell for INP-rich + INP-free particles

$N_{aer} = 300/cc$ (two-mode lognormal) $N_{INP} = 150/L$ (lognormal, $D_g = 0.74$ μm, $\sigma_g = 2.55$)

particle-based μ-physics + prescribed-flow test

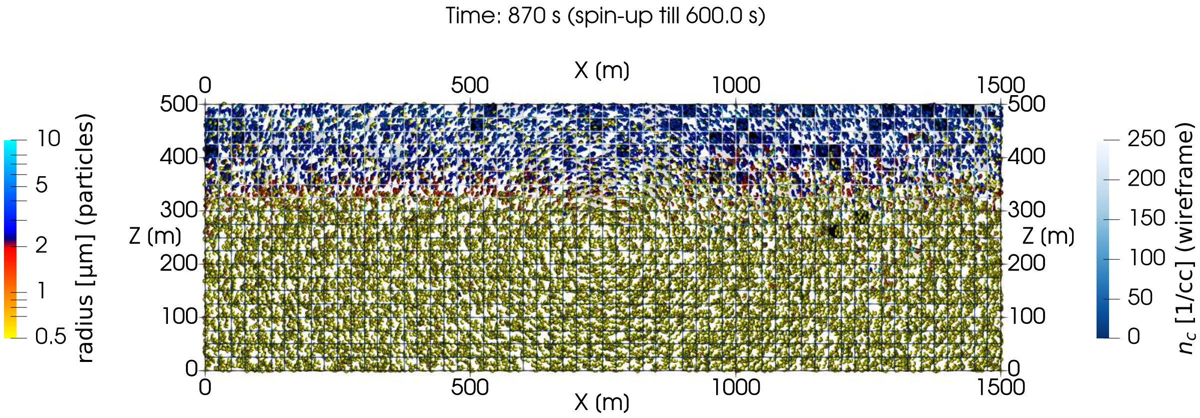

16+16 super-particles/cell for INP-rich + INP-free particles

$N_{\text{aer}} = 300/cc$ (two-mode lognormal) $N_{\text{INP}} = 150/L$ (lognormal, $D_g = 0.74\ \mu\text{m}$, $\sigma_g = 2.55$)

particle-based μ-physics + prescribed-flow test

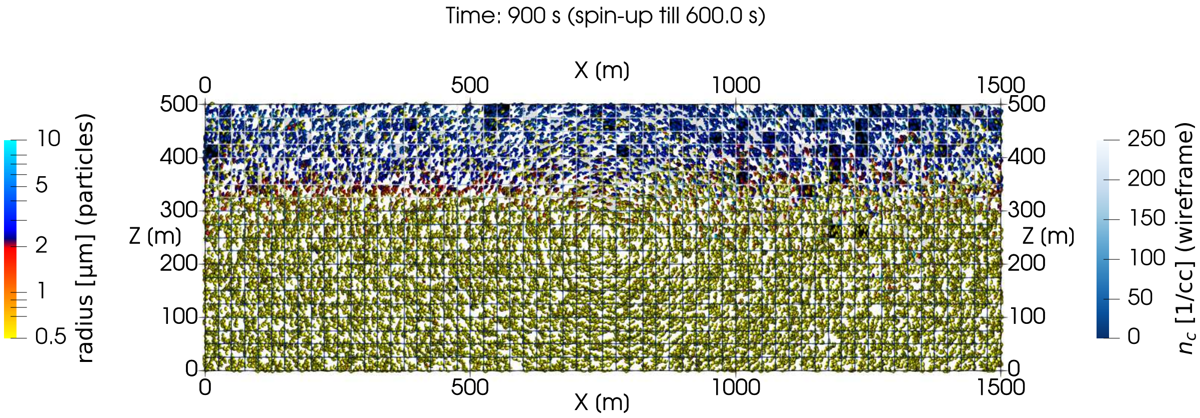

16+16 super-particles/cell for INP-rich + INP-free particles

$N_{\text{aer}} = 300/cc$ (two-mode lognormal) $N_{\text{INP}} = 150/L$ (lognormal, $D_g = 0.74\ \mu$m, $\sigma_g = 2.55$)

particle-based μ-physics + prescribed-flow test

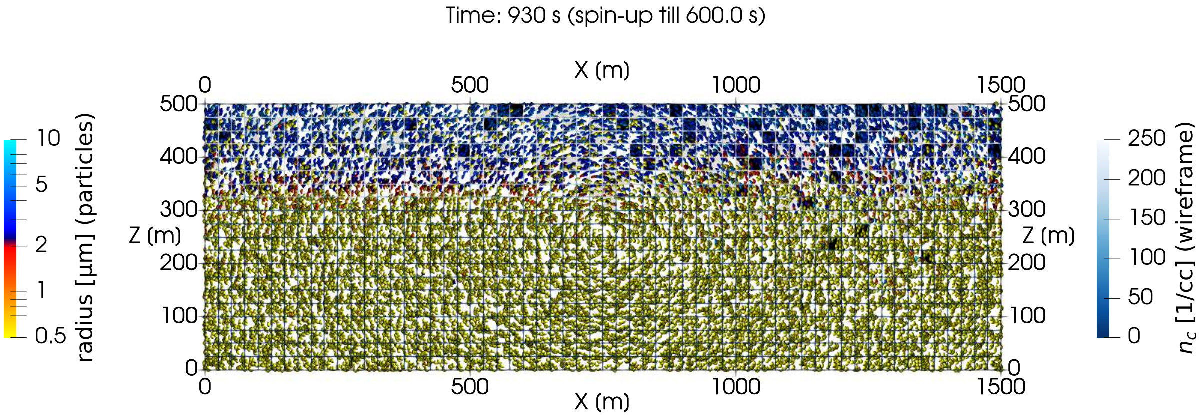

16+16 super-particles/cell for INP-rich + INP-free particles

$N_{\text{aer}} = 300/cc$ (two-mode lognormal) $N_{\text{INP}} = 150/L$ (lognormal, $D_g = 0.74\ \mu\text{m}$, $\sigma_g = 2.55$)

particle-based μ-physics + prescribed-flow test

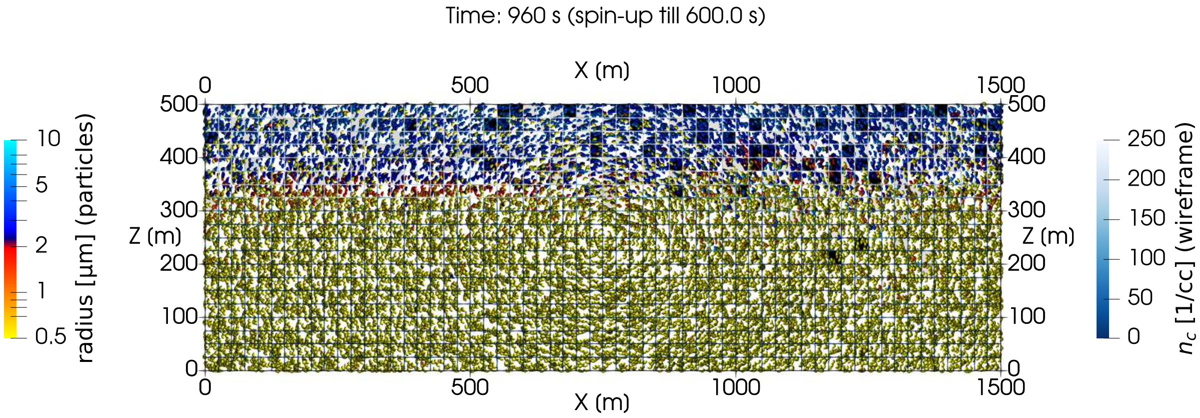

16+16 super-particles/cell for INP-rich + INP-free particles

$N_{aer} = 300/cc$ (two-mode lognormal) $N_{INP} = 150/L$ (lognormal, $D_g = 0.74\ \mu m$, $\sigma_g = 2.55$)

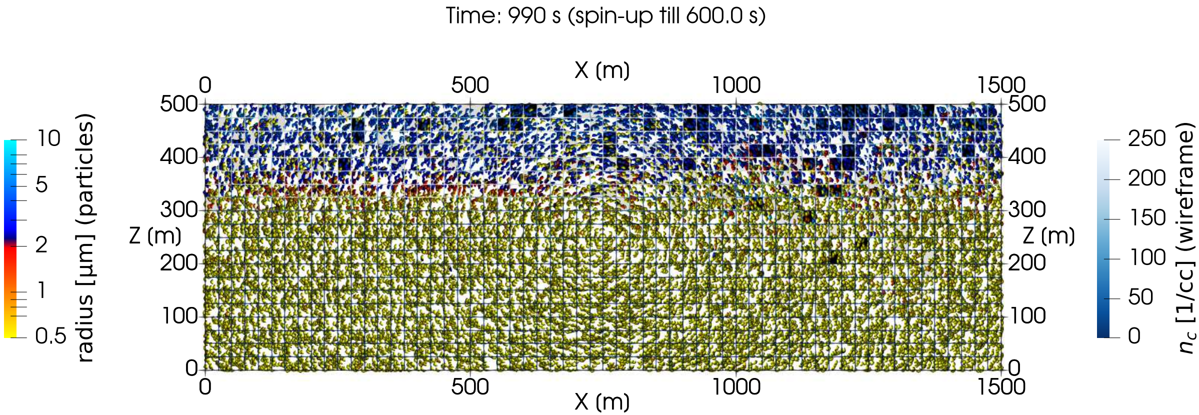

16+16 super-particles/cell for INP-rich + INP-free particles

N_{aer} = 300/cc (two-mode lognormal) N_{INP} = 150/L (lognormal, D_g = 0.74 μm, σ_g = 2.55)

particle-based μ-physics + prescribed-flow test

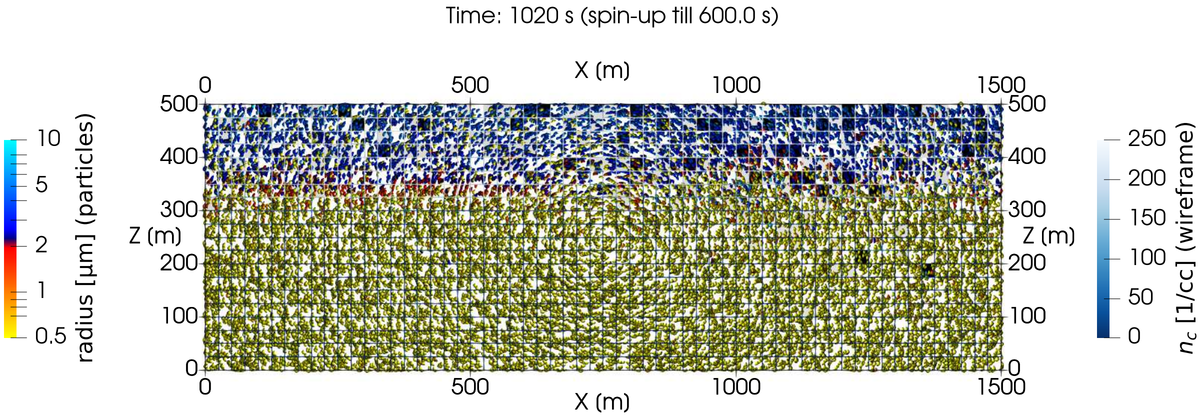

16+16 super-particles/cell for INP-rich + INP-free particles

$N_{aer} = 300/cc$ (two-mode lognormal) $N_{INP} = 150/L$ (lognormal, $D_g = 0.74\ \mu$m, $\sigma_g = 2.55$)

particle-based μ-physics + prescribed-flow test

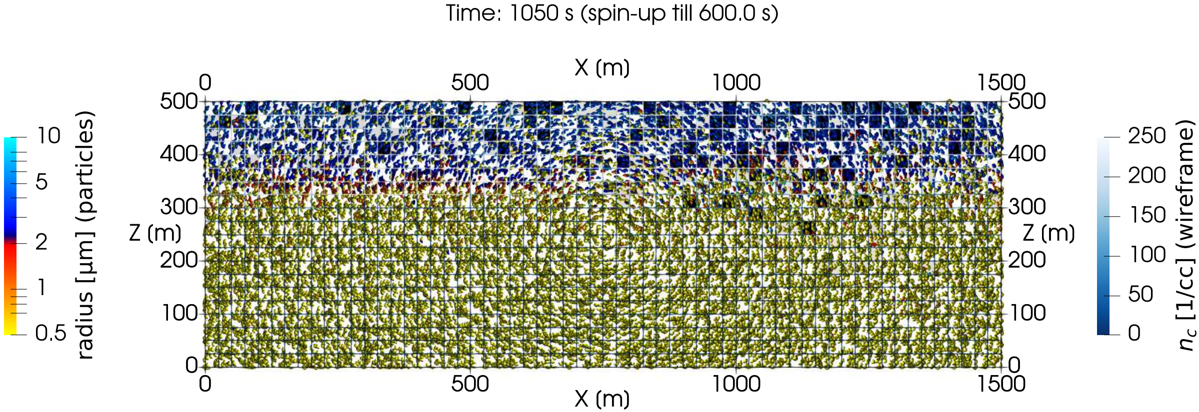

16+16 super-particles/cell for INP-rich + INP-free particles

$N_{\text{aer}} = 300/cc$ (two-mode lognormal) $N_{\text{INP}} = 150/L$ (lognormal, $D_g = 0.74\ \mu$m, $\sigma_g = 2.55$)

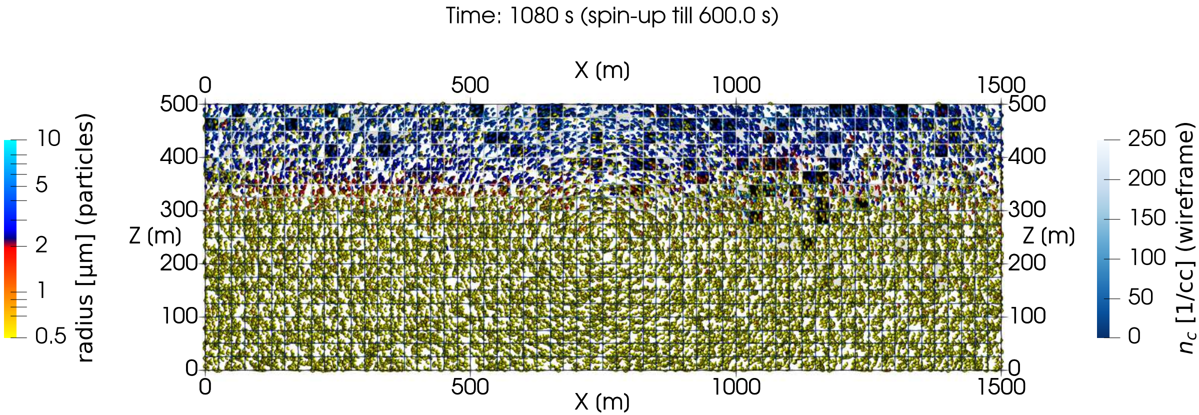

16+16 super-particles/cell for INP-rich + INP-free particles

$N_{aer} = 300/cc$ (two-mode lognormal) $N_{INP} = 150/L$ (lognormal, $D_g = 0.74$ μm, $\sigma_g = 2.55$)

particle-based μ-physics + prescribed-flow test

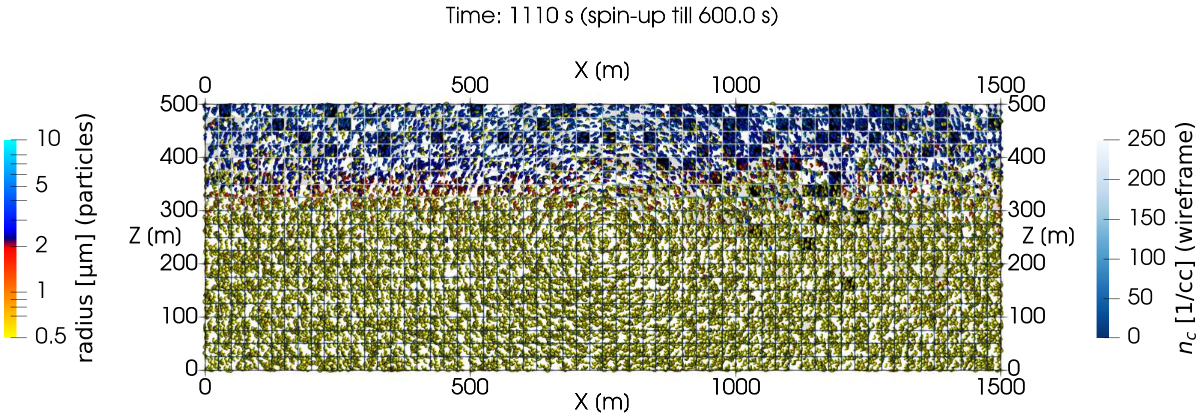

16+16 super-particles/cell for INP-rich + INP-free particles

$N_{aer} = 300/cc$ (two-mode lognormal) $N_{INP} = 150/L$ (lognormal, $D_g = 0.74\ \mu m$, $\sigma_g = 2.55$)

particle-based μ-physics + prescribed-flow test

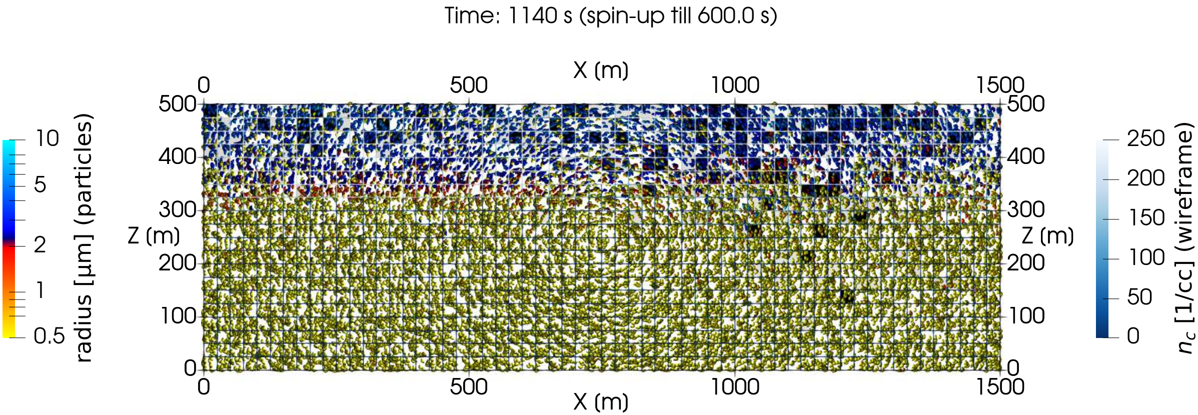

16+16 super-particles/cell for INP-rich + INP-free particles

$N_{\text{aer}} = 300/cc$ (two-mode lognormal) $N_{\text{INP}} = 150/L$ (lognormal, $D_g = 0.74\ \mu$m, $\sigma_g = 2.55$)

particle-based μ-physics + prescribed-flow test

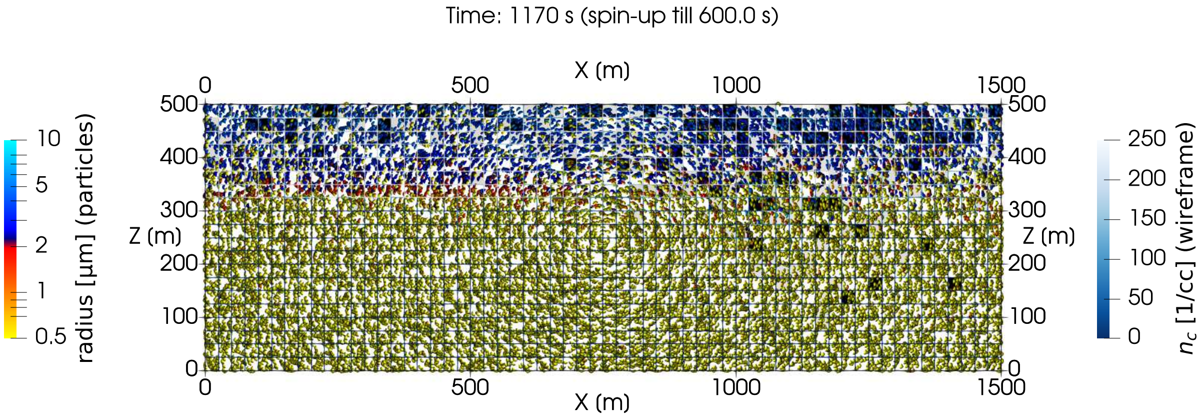

16+16 super-particles/cell for INP-rich + INP-free particles

$N_{aer} = 300/cc$ (two-mode lognormal) $N_{INP} = 150/L$ (lognormal, $D_g = 0.74\ \mu m$, $\sigma_g = 2.55$)

particle-based μ-physics + prescribed-flow test

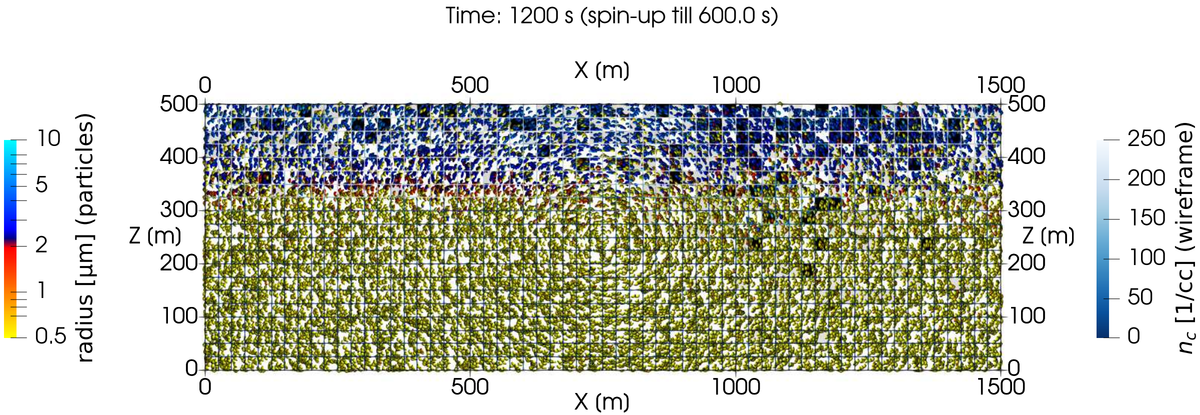

16+16 super-particles/cell for INP-rich + INP-free particles

$N_{\text{aer}} = 300/cc$ (two-mode lognormal) $N_{\text{INP}} = 150/L$ (lognormal, $D_g = 0.74$ μm, $\sigma_g = 2.55$)

testing three flow regimes and two immersion freezing representations

$w_{max} \approx 1/3$ m/s

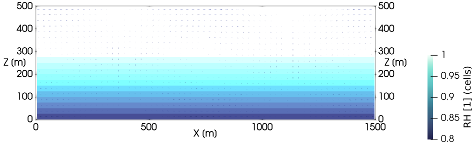

$w_{max} \approx 1$ m/s

$w_{max} \approx 3$ m/s

testing three flow regimes and two immersion freezing representations

$w_{max} \approx 1/3$ m/s

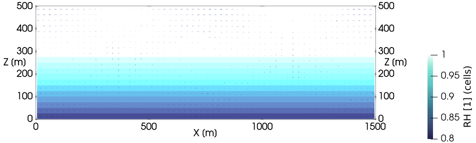

$w_{max} \approx 1$ m/s

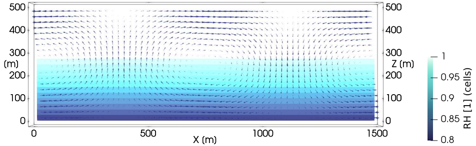

$w_{max} \approx 3$ m/s

testing three flow regimes and two immersion freezing representations

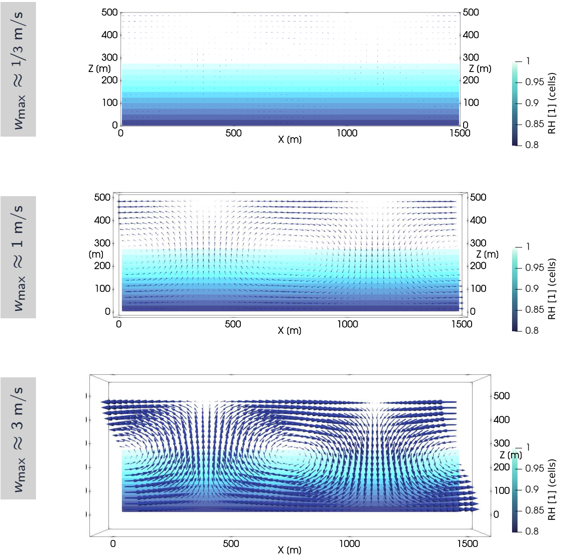

testing three flow regimes and two immersion freezing representations

$w_{max} \approx 1/3$ m/s

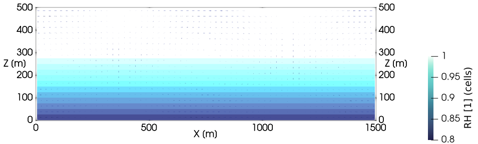

$w_{max} \approx 1$ m/s

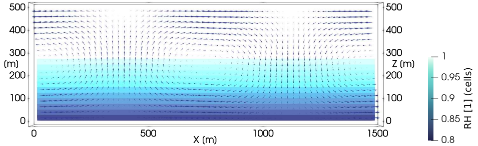

$w_{max} \approx 3$ m/s

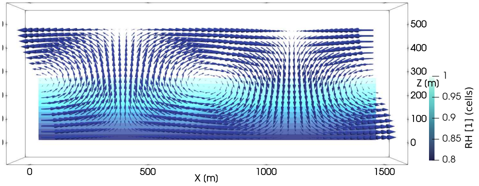

singular (INAS)

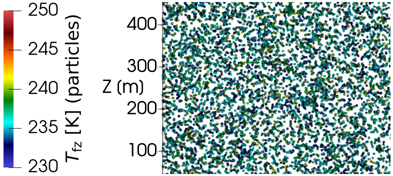

time-dependent (ABIFM)

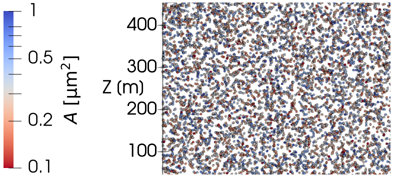

testing three flow regimes and two immersion freezing representations

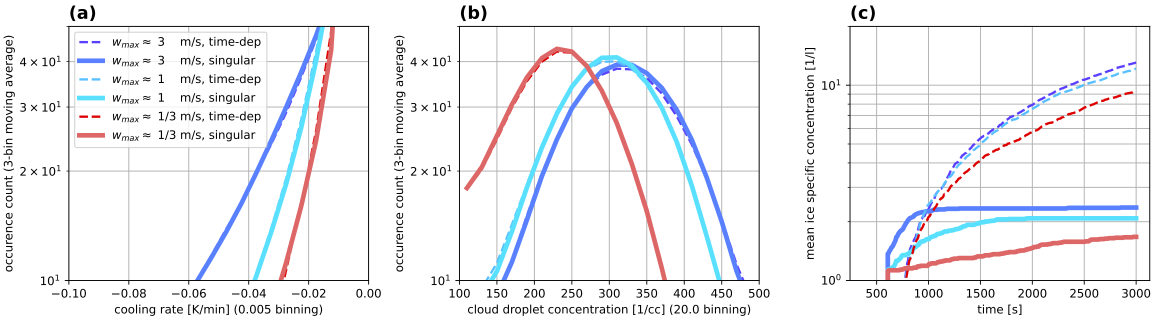

- range of cooling rates in simple flow (far from $c \sim 1$ K/min for AIDA as in Niemand et al. 2012)

testing three flow regimes and two immersion freezing representations

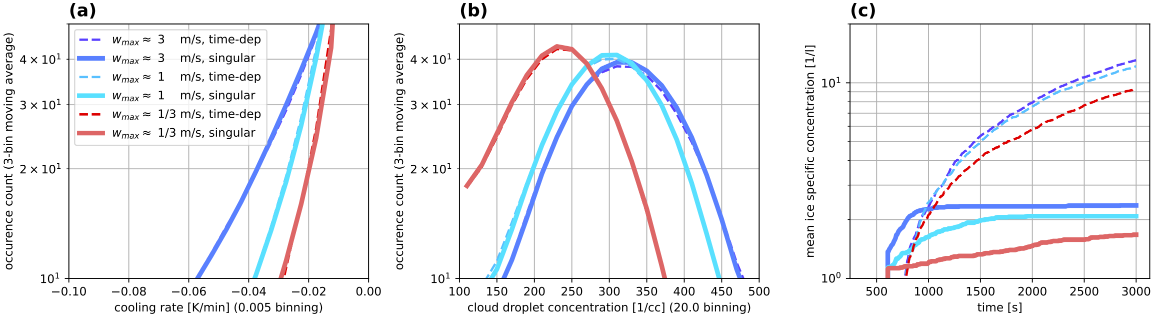

- range of cooling rates in simple flow (far from $c \sim 1$ K/min for AIDA as in Niemand et al. 2012)
- singular vs. time-dependent markedly different (consistent with box model for $c \ll 1K/min$)

testing three flow regimes and two immersion freezing representations

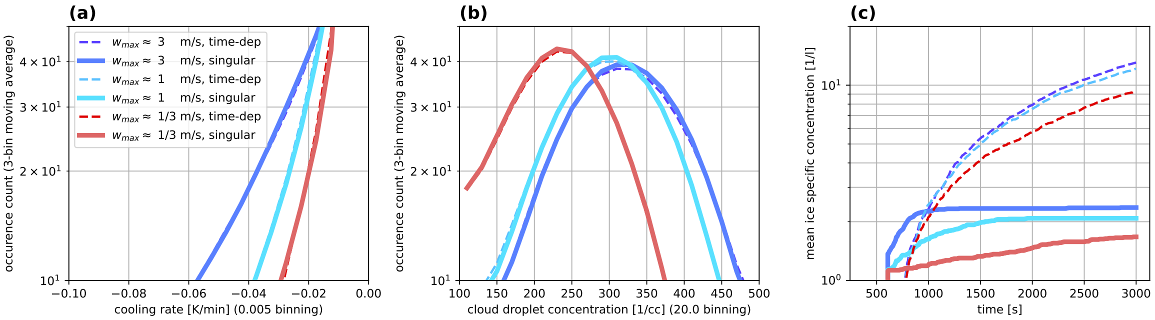

- range of cooling rates in simple flow (far from $c \sim 1$ K/min for AIDA as in Niemand et al. 2012)
- singular vs. time-dependent markedly different (consistent with box model for $c \ll 1K/min$)
- CPU time trade off: time dependent ca. 3-4 times costlier

- emergence of comprehensive mixed-phase particle-based aerosol/cloud/precip μ-physics models
  (Shima et al.; McSnow by Brdar, Siewert, Seifert et al.; Sölch, Kärcher, Unterstrasser et al. @DLR)
- probabilistic particle-based methods apt for stochastic processes: nucleation, collisions, breakup,...

- emergence of comprehensive mixed-phase particle-based aerosol/cloud/precip μ-physics models (Shima et al.; McSnow by Brdar, Siewert, Seifert et al.; Sölch, Kärcher, Unterstrasser et al. @DLR)
- probabilistic particle-based methods apt for stochastic processes: nucleation, collisions, breakup,...
- this study: **ABIFM-based time-dependent particle-based immersion freezing**

- emergence of comprehensive mixed-phase particle-based aerosol/cloud/precip μ-physics models
  (Shima et al.; McSnow by Brdar, Siewert, Seifert et al.; Sölch, Kärcher, Unterstrasser et al. @DLR)
- probabilistic particle-based methods apt for stochastic processes: nucleation, collisions, breakup,...
- this study: **ABIFM-based time-dependent particle-based immersion freezing**
  - box examples: role of INP size spectral width (same for time-dependent and singular)
  - box & 2D: cooling rate hardcoded in INAS fits $\rightsquigarrow$ limited robustness to different flow regimes
  - particle-based schemes (both singular and time-dependent) resolve INP reservoir

- emergence of comprehensive mixed-phase particle-based aerosol/cloud/precip μ-physics models (Shima et al.; McSnow by Brdar, Siewert, Seifert et al.; Sölch, Kärcher, Unterstrasser et al. @DLR)

- probabilistic particle-based methods apt for stochastic processes: nucleation, collisions, breakup,...

- this study: **ABIFM-based time-dependent particle-based immersion freezing**
  - box examples: role of INP size spectral width (same for time-dependent and singular)
  - box & 2D: cooling rate hardcoded in INAS fits $\rightsquigarrow$ limited robustness to different flow regimes
  - particle-based schemes (both singular and time-dependent) resolve INP reservoir

- next steps: leverage particle-resolved representation to simulate diverse INP populations

- emergence of comprehensive mixed-phase particle-based aerosol/cloud/precip μ-physics models (Shima et al.; McSnow by Brdar, Siewert, Seifert et al.; Sölch, Kärcher, Unterstrasser et al. @DLR)

- probabilistic particle-based methods apt for stochastic processes: nucleation, collisions, breakup,...

- this study: **ABIFM-based time-dependent particle-based immersion freezing**
  - box examples: role of INP size spectral width (same for time-dependent and singular)
  - box & 2D: cooling rate hardcoded in INAS fits $\rightsquigarrow$ limited robustness to different flow regimes
  - particle-based schemes (both singular and time-dependent) resolve INP reservoir

- next steps: leverage particle-resolved representation to simulate diverse INP populations

ASR Atmospheric System Research
DOE ASR grant no. DE-SC0021034

- emergence of comprehensive mixed-phase particle-based aerosol/cloud/precip μ-physics models (Shima et al.; McSnow by Brdar, Siewert, Seifert et al.; Sölch, Kärcher, Unterstrasser et al. @DLR)
- probabilistic particle-based methods apt for stochastic processes: nucleation, collisions, breakup,...
- this study: **ABIFM-based time-dependent particle-based immersion freezing**
  - box examples: role of INP size spectral width (same for time-dependent and singular)
  - box & 2D: cooling rate hardcoded in INAS fits $\rightsquigarrow$ limited robustness to different flow regimes
  - particle-based schemes (both singular and time-dependent) resolve INP reservoir
- next steps: leverage particle-resolved representation to simulate diverse INP populations

ASR Atmospheric System Research
DOE ASR grant no. DE-SC0021034

project hosted at: ILLINOIS

- emergence of comprehensive mixed-phase particle-based aerosol/cloud/precip μ-physics models (Shima et al.; McSnow by Brdar, Siewert, Seifert et al.; Sölch, Kärcher, Unterstrasser et al. @DLR)
- probabilistic particle-based methods apt for stochastic processes: nucleation, collisions, breakup,...
- this study: **ABIFM-based time-dependent particle-based immersion freezing**
  - box examples: role of INP size spectral width (same for time-dependent and singular)
  - box & 2D: cooling rate hardcoded in INAS fits $\rightsquigarrow$ limited robustness to different flow regimes
  - particle-based schemes (both singular and time-dependent) resolve INP reservoir
- next steps: leverage particle-resolved representation to simulate diverse INP populations

ASR Atmospheric System Research
DOE ASR grant no. DE-SC0021034

project hosted at: ILLINOIS

open python code: /atmos-cloud-sim-uj

- emergence of comprehensive mixed-phase particle-based aerosol/cloud/precip μ-physics models (Shima et al.; McSnow by Brdar, Siewert, Seifert et al.; Sölch, Kärcher, Unterstrasser et al. @DLR)

- probabilistic particle-based methods apt for stochastic processes: nucleation, collisions, breakup,...

- this study: **ABIFM-based time-dependent particle-based immersion freezing**
  - box examples: role of INP size spectral width (same for time-dependent and singular)
  - box & 2D: cooling rate hardcoded in INAS fits $\rightsquigarrow$ limited robustness to different flow regimes
  - particle-based schemes (both singular and time-dependent) resolve INP reservoir

- next steps: leverage particle-resolved representation to simulate diverse INP populations

ASR Atmospheric System Research | DOE ASR grant no. DE-SC0021034

project hosted at: ILLINOIS

open python code: /atmos-cloud-sim-uj

Thank you for your attention!